The Connection Between Multicomponent Smoluchowski's Equation, Multidimensional Inviscid Burgers' Equations and Random Graphs.

A thesis presented for the
Master's degree in Mathematical Sciences

Camillo Schenone

SUPERVISOR
Dr. Ivan Kryven

SECOND READER
Dr. Wioletta Ruszel

Utrecht University
March 2022

Abstract

We consider multicomponent Smoluchowski's coagulation equation with a bilinear kernel and mono-dispersed initial conditions. Because of the choice for the kernel, this equation maps to a partial differential equation called the inviscid Burgers' equation. We show in one-dimension, and claim it also holds in higher dimensions, that connected components in coloured Erdös-Renyi random graph asymptotically describe the solution to the Smoluchowski's equations for monodispersed intial conditions and the nonlinear PDE associated to it. Using Joyal's formalism of combinatorial species, we obtain a closed-form solution for these equations by counting connected components in the random graph. We also derive a simple equation for the blow up time of the Burgers' inviscid equation with the chosen bilinear form.

Using the insights obtained from our method, and adapting previous algorithms, we additionally propose a randomized numerical scheme that constructs d-coloured random graphs with N vertices and expected degree distribution in time $O((d+1)N)$. Using this algorithm we can inexpensively compute solutions to the multiplicative multicomponent Smoluchowski's equation (and consequently to Burgers' inviscid equation) at any time before solution blow up, hence resolving the curse of dimensionality for this problem.

Contents

Chapter 1

Introduction

> "*Coagulation and fragmentation belong to the most fundamental processes occurring in animate and inanimate matter. [...] Thus together with the Boltzmann equation that describes collision phenomena in rarefied gasses, and the Navier-Stokes and Euler equations modelling the flow of viscous fluids, the Smolushowski's equation is considered to be one of the most fundamental equations of the classical description of matter.*"
>
> — J. Banisiak, W. Lamb, P. Laurençon, *Analytic Methods for Coagulation-Fragmentation Models*

Coagulation and fragmentation are fundamental processes present in a plethora of scenarios that involve an identifiable population of animate or inanimate objects. These objects can coalesce together forming new entities or separating into smaller quantities. These are some of the simplest and most natural concepts in the physical world. It then comes without surprise that mathematicians took an interest in such processes and developed mathematical models to study them. What may although come as a surprise, is the fact that the earliest mathematical description of such a fundamental concept was pioneered by Marian von Smoluchowski only at the start of the XX century with the two papers [Smo27, Smo18] published in 1916 and 1917 respectively. He introduced an infinite system of discrete ordinary differential equations describing the evolution in time of clusters of atomic particles that through Brownian motion would end up close enough to create a connection and coalesce into a single cluster.

We call $w_k(t)$ the density of clusters of size k in the system at time t, and $K(x, y)$ the *aggregation kernel*, which describes the rate at which particles of size x aggregate with particles of size y. Then, the rate of change in time of the density of particles of size k, $\dot{w}_k(t)$ is given by:

$$\dot{w}_k(t) = \frac{1}{2}\sum_{s=1}^{k-1} K(s, k-s) w_s(t) w_{k-s}(t) - \sum_{s=1}^{\infty} K(s, k) w_s(t) w_k(t)\,. \tag{1.1}$$

Due to the broad applicability in applied physics and engineering, some close form solutions in very specific cases were obtained in the following years as well as some initial results on uniqueness and existence. However, a systematic and rigorous study of the subject did not commence until the 1980s. Albeit very intuitive in concept, it quickly became also clear the inherent difficulty of the subject [Lus73].

1.1 Review of Coalescence-like Processes

Coalescence is a process that acts on a number of small or atomic objects or entities. Every such object has one or more properties. In the monocomponent (or one-dimensional) case objects only have one property. In most physical treatments of the subject, the property of interest is often just the *mass* or *volume* of an object, as those are properties that have a more profound natural intuition in the context in which this subject evolved. In multicomponent analysis, objects will have multiple properties. A process on these atomic entities, then, is something that modifies their properties, making them evolve following different rules, which define the process itself.

In our context, coalescence is only a particular process that describes how two entities merge together to form a new object which has the sum of the properties of its constituents. But this is not the only possible process in this scenario, for example, there could be many different types of behaviours, which often arise from the natural world, but not exclusively:

- **Growth:** where we see infinitesimal elements slowly merge into an object, increasing its properties bit by bit [MB92, GL96].
- **Fragmentation:** (or Breakage) the separation of an object into two smaller ones [ILHE01, ADB09].
- **Nucleation:** the process that describes how infinitesimal elements in the environment can precipitate and add new objects to the system, often modelled as a source of particles [HRM88].
- **Coalescence:** (or Aggregation) when two objects merge together to form a bigger object [HRM88, KKPS93, LDG98].

Such processes arise in a plethora of natural phenomena, some of the most prominent are:

Aerosol Physics: An aerosol is when we have infinitesimal objects suspended in a gaseous environment. Such as liquid droplets or very fine solid particles dispersed in the atmosphere. The subject of aerosol physics finds many possible applications, from sand storm and volcanic dust modelling to cloud formation in the atmosphere or rain droplet formation, as well as desired industrial products and modelling the effects of undesired industrial by-products released into the atmosphere, a very contemporary topic [FM77, OKMO$^+$13, VR12, PK10, Dra72, SP16].

Planet and Star Formation: The primordial stage of stars and planets is a giant molecular cloud of dust-like particles. After an initial gravitational collapse which creates the core of a star the remaining dust flattens into a protoplanetary disc. The inner part of the latter will go on and collapse into the core, creating the star. The remainder will be the building material of future planets and asteroids. This model is known as the *nebular hypothesis*; and in the early 90s the existence of these protoplanetary discs was confirmed by direct imaging, thanks to the Hubble telescope. Clearly, gravity is the main contributor to these processes, but the orbiting dynamics of the dust discs creates the perfect environment for coagulation events of small scale objects (relative to the scale of a solar system, that means kilometers-sized solid objects) [BKB$^+$15, QS90, Lis93, Lee00, SYL99] .

Polymer Chemistry: Polymer chemistry is a clear cut example of application of a coagulation-fragmentation process. In the formation of a polymer we start from a solution of monomers, then we add monomers one by one until we obtain a desired long chain. Similarly, under stress or environmental changes, existing polymers can degrade and split up into smaller ones, in a process analogous to fragmentation [MB92].

Animal Groupings The fundamental nature of these processes makes them arise even in models where we are not dealing with inanimate objects but also in biological scenarios where we can observe animals forming groups, ranging from ants [Gor88] to dolphins and buffalo [OS78]. Coagulation-fragmentation processes attempt to explain the underlying mechanisms that lead to such groupings, and can be useful to better understand fish schooling [Niw98].

The first equations (1.1) proposed by Smoluchowski's were initially of discrete kind, with particles of integer positive mass and they only included aggregation terms. The model has since then been expanded and modified. Some of the modifications include the continuous models, with positive real-valued particles, introduced by Müller [Mül28] through the use of integro-differential equations. In addition, more complex equations have also been introduced to include decay phenomena of fragmentation [ILHE01, ADB09], or diffusion in which particles not only can merge but also break up or evaporate. Similarly, the model has been expanded to cater for a new type of dynamics such as *growth* [MB92, GL96], where infinitesimal objects adhere to already existing ones increasing their properties (i.e. sedimentation) or *nucleation* [HRM88] where infinitesimal objects dispersed in the environmental phase precipitate into new discrete small objects, effectively adding particles in the system. Naturally, development arose in an attempt to generalise the model to systems of multi-component particles. For example, an initial two variables study has been carried out in [Smi11, Wat06], where one variable is used for the mass and the other for its shape.

The seminal work of Smoluchowski was deterministic in nature, but, as already hinted, it had a stochastic argument at the root of its derivation. The markovian nature of the process underlying the model was quickly expanded into a probabilistic approach that developed in parallel to the deterministic model. First attempts at this approach were from Filippov [Fil61], Lushnikov [Lus78] and Marcus [Mar68], that introduced what is known as a Marcus-Lushnikov process. Stochastic approximations to the deterministic model are studied in [Bab99, Ber02, CF11, DFT02, EW01, FG04b, Nor99]. Questions of convergence of the stochastic Markov evolution of the system towards the deterministic coagulation equations also began to arise. Aldous [Ald99] actually proposed it as an open problem, solved then in [FG04a] under rather general conditions, extending the work of Norris [Nor99].

Most of the work has been done towards the monocomponent models for coagulation and fragmentation processes, thus, only interested in objects with a single property. What we have ignored so far, have been the multicomponent counterparts of these models, where the objects in question are aggregates of different types of "atoms" or molecules. Therefore, in multicomponent models, we are not only interested in how "big" an object is, but also in its composition, and we want to know how that composition evolves in time. This distinction has many useful applications and can lead to models that better predict subtler aspects of a range of natural and artificial processes. For example, the pharmaceutical powder excipient-active component study [MLK06], or the optical behaviour of aerosol in the atmosphere [BH98]. However, together with improving the capabilities of the model, generalising to multicomponent analysis comes with a significant increase in complexity in an already deceptively difficult problem. Nonetheless, a slew of results has been obtained in recent years, both numerical and analytical in nature. In [FLNV21b, FLNV21a] Ferreira *et al.* investigated the multicomponent Smoluchowski's coagulation equations under non-equilibrium stationary conditions assuming a source of small particles constantly being added to the system. In the continuous case, exact solutions for generic additive and product kernels, depending only on the mass of the aggregating objects, have been found [FDGG07, FDGG10]. In an attempt to curb the intrinsic curse of dimensionality of this problem, powerful numerical methods have been proposed [Ahr20, MZTS16].

The strong physical connection of these examples might tempt the reader to think that such processes are relegated as mere models of the physical world, and the temptation to only use names such as particles, molecules, and mass is strong. However, it is important to stress that the concepts treated here are much more general, and can be applied in much more abstract scenarios, where objects and entities are not necessarily material. To be consistent with this remark, we will try to maintain a neutral nomenclature throughout the manuscript. However, the physical intuition of the process is so natural that, sometimes, the nomenclature will reflect that.

1.2 Research Question

Continuing the work done so far by the scientific community, that reflects the importance of the subject, in this research we propose an analysis of the discrete multicomponent Smoluchowski's coagulation equations with composition-aware kernels, opposed to mass-only kernels approaches, found in the literature. The analysis will be carried out from a stochastic approach, using a conjectured connection with random graphs. Lastly, we will explore possible connections to the inviscid Burgers' equation, an example of a non-linear partial differential equation of particular interest, since it represents a very simple form of the notoriously difficult to analyse Navier-Stokes equation [LCT49], and is often used as a prototype for non-linear behaviour.

1.3 Main Results

In this manuscript, we will analyse the Smoluchowski's Coagulation Equation (1.1) and its connections with both PDEs and Random Graphs. The possibilities are many, and completely generic treatment of the subject would be inadvisable. In this script, we will only focus on the process of discrete symmetric Coalescence. Even with this initial simplification, the general subject remains very intractable and generously outside the capabilities of the author. Therefore we will assume a couple more simplifications that will hold throughout the manuscript. The first one will be related to the frequency and the modes with which the process evolves in time, by only focusing on the *multiplicative kernel* $K(r,s) = rs$. The second one is related to the starting state of the system. Indeed, most of the results that follow, only hold for the case of *monodisperse initial conditions*, that is to say, we always start from a system in which only atomic objects are present, and there haven't been any coagulations yet.

In Chapter 2 we lay the one-dimensional groundwork and a motivating example from which we will build upon in later chapters. In the following chapters, we will provide the three main results of this thesis.

In Chapter 3 we will propose and derive a model for d-dimensional multicomponent coalescence with a generalised non-diagonal product kernel that depends on the composition of the objects involved.

$$\dot{w}_{\mathbf{k}} = \frac{1}{2} \sum_{\mathbf{x}+\mathbf{y}=\mathbf{k}} w_{\mathbf{x}} w_{\mathbf{y}} \mathbf{x}^T A \mathbf{y} - \sum_{\mathbf{x}\in\mathbb{N}_0^d} w_{\mathbf{x}} w_{\mathbf{k}} \mathbf{x}^T A \mathbf{k} \quad \forall \mathbf{k} \in \mathbb{N}_0^d ,$$

where $K(\mathbf{x},\mathbf{y}) = \mathbf{x}^T A \mathbf{y}$ for some symmetric matrix A with non-negative entries, and

$$w_{\mathbf{k}} = w_{k_1,k_2,\ldots,k_d} , \quad k_i \in \mathbb{N}_0, \quad \forall i \in \{1,\ldots,d\}$$

denotes a multindex notation for the densities of objects made up of k_i elements of type i for every i.

In the literature, most multicomponent studies deal with diagonal kernels that are agnostic to the composition of the objects involved and are only dependent on their sizes. We will also find parallelisms with a multidimensional version of the inviscid Burgers' equation, (where $\mathbf{J}_U$ denotes the Jacobian matrix of U)

$$U_t = -\mathbf{J}_U A(U - M)\,,$$

which is of scientific interest as it is a very simple form of the Navier-Stokes equation in the Cartesian, time-dependent, compressible, limit [LCT49]. Finally, we will prove that under our specific assumptions, the blow up time for the multicomponent coalescence process is given by

$$t_c = \frac{1}{\|A\|}\,.$$

In Chapter 4, we will show how we can map the model just defined into a system of algebraic equations of generating functions using Joyal formalism, and which can be solved directly through the Goods' multidimensional generalisation of the Lagrange Inversion Theorem.

Lastly, in Chapter 5, we will use the insights obtained through the previous chapters to adapt an algorithm to construct pseudo Chung-Lu random graphs, which will allow us to generate d-coloured random graphs in $O((d+1)N)$ time instead of $O(N^d)$ of the naive case, here N is the number of nodes in the graph. We then can use this algorithm to generate graphs and *read out* the solution to the Smoluchowski's ODE system of coalescence equations.

Chapter 2

Monocomponent Coalescence

In this chapter, we will treat the one-dimensional case. We will initially solve the one-dimensional Smoluchowski's equation (1.1) through classical analytical means. We will then prove in one dimension that we can solve the system also through random graphs and that the two solutions match.

2.1 Deterministic Model with Multiplicative Kernel

As we said in the introduction, the process of coalescence is described by the merging of two entities, and the summation of their properties. To simplify the notations, in this case, the value of the property itself will also represent the object. Since we are in a discreet context, properties will be integer-valued, and for the remainder of the chapter, they will also be assumed to only be positive. Let r and s be two objects with property value r and s respectively. Then the coalescence process can be described by the following diagram:

$$\{r, s\} \to \{r + s\}\,.$$

The immediate next question is asking if and how properties of the objects involved in the coagulation influence the coagulation process itself. This aspect of the process is encapsulated in the *coalescence kernel* $K(r, s)$ (or *aggregation kernel*). Through the coalescence kernel we can arbitrarily define how often a specific configuration of two objects will merge together. We can enforce different types of processes, some of the most analytically tractable (yet still not trivial) are

- $K(r, s) = 1$ constant kernel, objects coalesce independent of their properties.
- $K(r, s) = r + s$ additive kernel.
- $K(r, s) = rs$ multiplicative kernel.

But kernels can also take on more complex shapes:

$$K(r, s) = (r^{1/3} + s^{1/3})(r^{-1/3} + s^{-1/3})\,.$$

These more complex kernels often arise from empirical observations in experimental applications. As previously mentioned, the focus will be towards the *multiplicative kernel*, which gives rise to non-linear dynamics.

Let us indicate with $w_k(t)$ the density of objects with property k at time t. Then, we model the number of coagulations $\{r, s\} \to \{r + s\}$ in a given time interval as

$$\frac{1}{2} w_r(t) w_s(t) K(r, s)\,.$$

Here we used the general assumption that the process is understood to be commutative. Therefore, the $1/2$ term is due to the symmetry of the transformations

$$\{r, s\} \to \{r + s\} \qquad \text{and} \qquad \{s, r\} \to \{s + r\}\,,$$

which both produce an object of the same cumulative property at the same rate due to assuming $K(r, s) = K(s, r)$. Of course in our specific case $K(s, r) = sr$, these considerations are obvious.

Consider all the coalescence events that result in an object with property k,

$$\frac{1}{2} \sum_{s=1}^{k-1} K(s, k - s) w_s w_{k-s}\,,$$

and all the events that involve objects of property k,

$$\sum_{s=1}^{\infty} K(s, k) w_s w_k\,.$$

If we merge these two quantities together with the correct signs, they describe a set of differential equations describing the rate of change of $w_k(t)$ in time, known as the *Smoluchowski's coagulation equations*:

$$\dot{w}_k = \frac{1}{2} \sum_{s=1}^{k-1} K(s, k - s) w_s w_{k-s} - \sum_{s=1}^{\infty} K(s, k) w_s w_k\,.$$

Which can be rewritten, with the knowledge that our kernel is the multiplicative one, as

$$\dot{w}_k = \frac{1}{2} \sum_{s+r=k} sr w_s w_r - k w_k \sum_{s=1}^{\infty} s w_s \quad \forall k \geq 1\,, \tag{2.1}$$

with the sum over $s, r \in \mathbb{N}$ representing a convolution. We define

$$M(t) := \sum_{s \in \mathbb{N}} s w_s(t)$$

as total amount of objects in the system.

2.1.1 Solving the model

The one dimensional multiplicative kernel, with monodisperse initial conditions, is one of those simple enough cases where we can find an explicit analytical solution to the system in the classical sense. We begin by defining the generating function for the cluster distribution

$$G(z,t) = \sum_{k=1}^{\infty} w_k(t) e^{-kz} .$$

The monodisperse initial condition assumption tells us that we will only have objects of size 1,

$$w_k(0) = \delta_{k,1} .$$

Remark. For now we are considering the series $G(z,t)$ as a pure algebraic object, without worries of convergence. However, we will need to treat them as functions. Therefore, we will assume

$$\sum_{k=1}^{\infty} k^2 w_k(t) < \infty .$$

Theorem 2.1.1. *Given a system of ODEs such as the one defined by (2.1) subjected to monodisperse initial conditions defined as above, then for $t \in [0,1)$,*

$$w_k(t) = \frac{k^{k-3} t^{k-1} e^{-kt}}{(k-1)!} \quad \forall k \geq 1$$

is the unique solution

Proof. The formal partial derivative of G with respect to z gives us

$$\frac{\partial}{\partial z} G(z,t) = \sum_{s>0} w_s(t) \frac{\partial}{\partial z} e^{-sz} = -\sum_{s>0} s w_s(t) e^{-sz} , \tag{2.2}$$

which if evaluated at $z = 0$ we get $G_z(0,t) = -M(t)$. This will come useful later.

We are interested in the evolution in time of $G(z,t)$ therefore we have

$$\begin{aligned}
\frac{\partial}{\partial t} G(z,t) &= \sum_{k>0} \dot{w}_k e^{-kz} && \text{substituting (2.1)} && (2.3)\\
&= \frac{1}{2} \sum_{k>0} \sum_{r+s=k} r s w_r w_s e^{-kz} - M(t) \sum_{k>0} k w_k e^{-kz} && && (2.4)\\
&= \frac{1}{2} \sum_{k>0} \sum_{r+s=k} r s w_r w_s e^{-(r+s)z} + M(t) G_z(z,t) && \text{from (2.2)} && (2.5)\\
&= \frac{1}{2} \left(\sum_{r>0} r w_r e^{-rz} \right) \left(\sum_{s>0} s w_s e^{-sz} \right) + M(t) G_z(z,t) && && (2.6)\\
&= \frac{1}{2} G_z(z,t)^2 + M(t) G_z(z,t) . && && (2.7)
\end{aligned}$$

Let now define $u(z,t) = -G_z(z,t)$ and proceed by finding

$$\frac{\partial}{\partial t}u = -\frac{\partial}{\partial t}G_z = \sum_{k>0} k\dot{w}_k e^{-kz} \tag{2.8}$$

$$= \frac{1}{2}\sum_{k>0}\sum_{r+s=k} krsw_r w_s e^{-kz} - M(t)\sum_{k>0} k^2 w_k e^{-kz} \tag{2.9}$$

$$= \frac{1}{2}\sum_{k>0}\sum_{r+s=k} (r+s)rsw_r w_s e^{-(r+s)z} + M(t)u_z \tag{2.10}$$

$$= \frac{1}{2}\sum_{k>0}\sum_{r+s=k} \left[r^2 s w_s w_r + r s^2 w_s w_r\right] e^{-(r+s)z} + M(t)u_z \tag{2.11}$$

$$= \frac{1}{2}\sum_{k>0}\sum_{r+s=k} \left[\left(r^2 w_r e^{-rz}\right)\left(s w_s e^{-sz}\right) + \left(r w_r e^{-rz}\right)\left(s^2 w_s e^{-sz}\right)\right] + M(t)u_z \tag{2.12}$$

$$= \frac{1}{2}\Bigg[\left(\sum_{r>0} r^2 w_r e^{-rz}\right)\left(\sum_{s>0} s w_s e^{-sz}\right) \tag{2.13}$$

$$+ \left(\sum_{r>0} r w_r e^{-rz}\right)\left(\sum_{s>0} s^2 w_s e^{-sz}\right)\Bigg] + M(t)u_z \tag{2.14}$$

$$= \frac{1}{2}[-u_z u - u u_z] + M(t)u_z \tag{2.15}$$

$$= -u_z u + M(t)u_z\,. \tag{2.16}$$

which describes an inviscid Burgers' equation that can be solved through the method of characteristics subjected to the initial conditions $u(z,0) = e^{-z}$, which correspond to the case of monodisperse initial conditions $w_k(0) = \delta_{k,1}$. The initial value problem

$$u_t + (u - M(t))u_z = 0 \quad u(z,0) = e^{-z} \tag{2.17}$$

has characteristic curves defined by

$$\frac{dz}{dt} = u - M \quad \text{and} \quad \frac{du}{dt} = 0\,.$$

From the first ODE we obtain

$$z(t) = tu - \int_0^t M(\tau)d\tau + \phi(u)\,,$$

and if we plug the initial conditions for $t = 0$ we get

$$z(0) = \phi(u(z(0),0)) = \phi(e^{-z(0)})\,,$$

therefore giving us the solution with $\phi(u) = -\log u$

$$z = tu - \log\, u - \int_0^t M(\tau)d\tau\,. \tag{2.18}$$

Thus, we can find u_z with

$$\frac{\partial}{\partial z}z = \frac{\partial}{\partial z}[tu - \log\, u - \int_0^t M(\tau)d\tau] = tu_z - \frac{1}{u}u_z\,,$$

which gives

$$u_z = -\frac{u}{1-tu}\,. \tag{2.19}$$

From the characteristics system we obtain in particular that $du/dt = 0$ and therefore

$$M(t) = -G_z(0,t) = u(0,t)\,. \tag{2.20}$$

In this proof we will focus solely on the time window $t < t_c$, where t_c is the critical time where we develop a singularity in the solution. Here we have that $\dot{M} = 0$ and $u(0,t) = M(t) = M(0) = 1$ from the initial conditions. This turns (2.18) into

$$z = tu - \log\, u - t\,. \tag{2.21}$$

In this regime we have that for $z = 0$ equation (2.19) becomes

$$u_z(0,t) = -\frac{u(0,t)}{1-tu(0,t)} = \frac{1}{1-t}\,,$$

which exhibit a singularity for $t \nearrow 1$. Hence

$$t_c = 1\,,$$

where the system undergoes a phase transition as the second moment of the generating function $-u_z(0,t) = G_{zz}(0,t)$ becomes unbounded.

We rewrite the expression (2.21) and obtain:

$$e^{-z} = ue^{t(1-u)}\,,$$

and finally we can extract the coefficients of $u(z,t) = \sum_k kw_k e^{-kz}$ via Lagrange expansion

$$\begin{aligned} u(z,t) &= \sum_{k>0}\frac{1}{k!}\left[\lim_{u\to 0}\frac{d^{k-1}}{du^{k-1}}(e^{t(u-1)})\right]e^{-kz} \\ &= \sum_{k>0}\frac{1}{k!}(kt)^{k-1}e^{-kt}e^{-kz}\,, \end{aligned}$$

therefore

$$[e^{-kz}]u(z,t) = kw_k(t) = \frac{k^{k-2}t^{k-1}e^{-kt}}{(k-1)!}\,,$$

so

$$w_k(t) = \frac{k^{k-3}t^{k-1}e^{-kt}}{(k-1)!}\,.$$

□

Corollary 2.1.2. *The solution to the system (2.1) converges to*

$$w_k(t) = \frac{1}{\sqrt{2\pi}} \frac{t^k e^{k(1-t)}}{tk^{5/2}},$$

for large k

Proof. Apply Stirling's approximation to the solution obtained in the last theorem. □

2.2 Random Graphs

In the last Section, we have looked at a model in which we describe how two objects with properties r and s join together to form a new object with a cumulative property of $r+s$, in a random coalescence processes. Up until now, we actively used a neutral nomenclature for the subjects of this discussion, partly not to spoil too much what will follow, but also to accentuate the jump. We have been talking, very generically, about objects with a certain property value. Which are made up of a collection of small entities which we will call, to make use of the physical nomenclature, *atomics*. If we begin to swap names around, and instead of objects we say "clusters" or even "connected components" and instead of monomers, we say "nodes", hopefully the hint is strong enough to introduce what is to come. There is an almost natural interpretation of a random coalescence process through the lenses of a random graph. Can the statistics of the connected components in a random graph describe the evolution of the clusters in a random coalescence process?

One first complication with random graphs is that they are discrete objects while the classical approach follows a continuous-time evolution. The hope is that by taking big enough graphs with $n \to \infty$ we will be able to bridge this gap.

2.2.1 Erdös-Rényi random graphs

In the Erdös-Renyi random graph $G(n,p)$ model there are n vertices and all $\binom{n}{2}$ edges have an independent probability p of being present. In their original work [ER59] the model was defined as $G(n,e)$, describing the state of the graph with n nodes after e edges had been added uniformly at random. Today, it is preferred the notation $G(n,p)$, and it can be proven that $G(n,e)$ and $G(n,p)$ with $e = p\binom{n}{2}$ describe the same distribution of graphs. As we add more and more edges, once we reach and pass $e = n/2$ edges, the model undergoes a phase transition, where a giant component emerges [Spe09]. This is one of the most striking facts about the Erdös-Renyi model, and partly one of the reasons for its success. By parametrising the probability with $p = c/n$ we obtain that the critical case of $e = n/2$ happens for $c = \frac{n}{n-1}$. In the large n limit, c will converge towards one. For the sake of simplicity we will limit ourselves to selecting $c = 1$ as the critical value. However, it is useful to keep in mind, especially when performing finite simulations, that the actual critical parameter is always an ε more than 1.

From the initial work of Erdös and Renyi we know that such graphs have 3 different windows of behaviour: (these windows can be refined into 5, but this is outside the scope of this section, for details more informations can be found in [AS00])

- **subcritical:** $c < 1$, all the components are tree like and very small $O(\ln n)$.
- **critical:** $c = 1$, the critical window of complex behaviour giant component size is $O(n^{2/3})$.
- **supercritical:** $c > 1$, we have a giant component of increasing complexity as c increases and of substantial scale, all other components remain small.

In this discussion we will be focusing entirely in the subcritical window.

Assume now, that for each n we get an associated graph $G(n, p_n)$ where p_n is defined such that it is convergent

$$\lim_{n\to\infty} np_n = c \tag{2.22}$$

for all n. This way we decouple from the number of nodes as a discriminating parameter and all graphs have the same behaviour independently on the exact amount of nodes we consider. We can write directly $G(n, c)$ for some $c \in [0, 1)$.

The degree distribution for Erdös-Renyi random graphs is binomial, that is

$$d(k) = \binom{n-1}{k} p^k (1-p)^{n-1-k}. \tag{2.23}$$

Given that we are choosing p_n such that to keep $c = np_n$ constant, then we can see that this binomial distribution converges to a Poisson distribution with parameter c as n increases

$$\begin{aligned}
\lim_{n\to\infty} d_k &= \lim_{n\to\infty} \binom{n-1}{k} p^k (1-p)^{n-1-k} && (2.24)\\
&= \lim_{n\to\infty} \frac{(n-1)(n-2)\dots(n-k)}{k!} p^k (1-p)^{n-1-k} && (2.25)\\
&= \lim_{n\to\infty} \frac{n^k}{k!} (1-\frac{c}{n})^n \left[(1-\frac{1}{n})\dots(1-\frac{k}{n})\right] (\frac{c}{n})^k \frac{1}{(1-p)^{1+k}} && (2.26)\\
&= \frac{c^k}{k!} e^{-c}. && (2.27)
\end{aligned}$$

Fix now a $c \in [0, 1]$, define as $S^{(n)}(c)$ the set of connected components of $G(n, c)$, then we define $P_k^{(n)}(c)$ as

$$P_k^{(n)}(c) = \frac{|\{s : |s| = k, s \in S^{(n)}(c)\}|}{|S^{(n)}(c)|} \quad \text{and} \quad P_k(c) = \lim_{n\to\infty} P_k^{(n)}(c). \tag{2.28}$$

or in words, the probability of selecting a connected component of size k when choosing uniformly at random from $S^{(n)}(c)$, and the corresponding limiting probability. We already said that the topology of the graph mainly depends on c, and consequently also its connected components will depend only on it. We can then define the normalised density $\tilde{w}_k(c)$ of components of size k in the Erdös-Renyi setting as

$$\tilde{w}_k(c) = \lim_{n\to\infty} \frac{|\{s : |s| = k, s \in S^{(n)}(c)\}|}{n} \tag{2.29}$$

$$= \lim_{n\to\infty} \frac{|\{s : |s| = k, s \in S^{(n)}(c)\}|}{\sum_m m|\{s : |s| = m, s \in S^{(n)}(c)\}|} \tag{2.30}$$

$$= \lim_{n\to\infty} \frac{P_k^{(n)}(c)|S^{(n)}(c)|}{|S^{(n)}(c)|\sum_m mP_m^{(n)}(c)} = \frac{P_k(c)}{\sum_k kP_k(c)}\,. \tag{2.31}$$

We will now show that these two quantities, so intuitively close together, are indeed the same.

Theorem 2.2.1. *Let $c \in [0, 1)$, and $P_k^{(n)}(c)$ be the density of connected components of size k in an Erdös-Renyi random graph with n nodes $G(n, c/n)$. Then*

$$\tilde{w}_k(c) = \lim_{n\to\infty} \frac{P_k^{(n)}(c)}{\sum_k kP_k^{(n)}(c)} = w_k(c)\,,$$

where $w_k(c)$ is the solution to (2.1) for monodisperse initial conditions $w_k(0) = \delta_{k,1}$

In other words, for each t, the distribution of sizes of the connected components of an Erdös-Renyi random graph $G(n, t/n)$ converges to the solution $w_k(t)$ to the Smoluchowski's equations for monodisperse initial conditions. We will prove this theorem after defining some important results that will also be useful in the next sections.

2.2.2 Lagrange inversion

Lagrange inversion formula is a classical tool for coefficient extraction from series. For a thorough treatment of most of the results and definitions we refer to [BLL97].

Theorem 2.2.2. *Let $H(x, y)$ be a series in x, y in the ring $\mathbb{A}[x, y]$ of formal power series, satisfying*

$$H(0, 0) = 0 \qquad \text{and} \qquad \frac{\partial H}{\partial y}(0, 0) = 0\,,$$

then the implicit functional equation

$$A(x) = H(x, A(x))$$

uniquely characterises the series $A(x)$ for which $A(0) = 0$

Corollary 2.2.3. *Let $A(x)$ and $R(x)$ be two series in the ring $\mathbb{A}[x]$ of formal power series, then the implicit functional equation*

$$A(x) = xR(A(x))$$

has an unique solution $A(x)$.

Theorem 2.2.4. *Let $A(x), R(x)$ be formal power series in $\mathbb{A}[x]$ such that*

$$A(x) = xR\left[A(x)\right] ,$$

then for any formal power series $F(x)$ we have

$$[x^n]F\left[A(x)\right] = \frac{1}{n}[t^{n-1}]F'(t)R^n(t) .$$

Moreover, we know that in the subcritical regime ($c < 1$) connected components of an Erdös-Renyi random graph are all simple and locally tree-like [BR15] and a theorem stated in [AS00] says that

Theorem 2.2.5. *given positive real c and positive integer k*

$$\lim_{n\to\infty} \mathbb{P}(|s| = k \text{ in } G(n,c)) = \mathbb{P}(T_c = k) ,$$

where T_c is the total size of a Galton-Watson process using Poisson distribution with mean c. And where s is a connected component of $G(n,c)$.

We can now use these results to prove Theorem 2.2.1.

Proof. Thanks to Theorem 2.2.5, we know that as n increases, the connected components of an Erdös-Renyi random graph converges to random trees with Poisson offspring distribution. Let $W(z)$ be the formal power series representing the total progeny distribution of the Poisson trees and $U(z)$ be the generating function for the degree distribution of $G(n,c)$, which we know to converge to a Poisson distribution in the big n limit. Following [Kry17], we can setup a system of implicit algebraic equations

$$\begin{cases} W(z) = zU(W'(z)) \\ W'(z) = zU'(W'(z)) \end{cases} , \tag{2.32}$$

where U' and W' represent the generating functions for the excess distributions generated by U and W, respectively.

We know in this case that $U(z)$ is the generating function for the Poisson distribution, and therefore $U'(z) = U(z)$. Reducing the system to

$$W(z) = zU(W(z)) . \tag{2.33}$$

Using 2.2.4 we can extract the coefficient of W obtaining

$$[z^n]W(z) = \frac{1}{n}[s^{n-1}]U^n(s) . \tag{2.34}$$

Recalling once more that $U(s) = e^{c(1-s)}$ and $U^n(s) = e^{nc(1-s)}$ we finally obtain that

$$[z^k]W(z) = \frac{1}{k} e^{-ck} [s^{k-1}] \sum_{m>0} \frac{(kc)^m}{m!} s^m = \frac{1}{k} \frac{(kc)^{k-1} e^{-kc}}{(k-1)!} \,. \tag{2.35}$$

Lastly, since W generates the total progeny of a tree, it represents the number of nodes that make up components of that size, that is $k\tilde{w}_k(c)$, so finally

$$\tilde{w}_k(c) = \frac{1}{k^2} \frac{(kc)^{k-1} e^{-kc}}{(k-1)!} = \frac{k^{k-3} c^{k-2} e^{-kc}}{(k-1)!} = w_k(c) \,. \tag{2.36}$$

□

Therefore, we can match the solution obtained in the previous sections through more classical methods. As an added bonus, we also obtain that we can read off random graphs components to find particular solutions to a non-linear partial differential equation, such as the Burgers' equation.

Chapter 3

Multicomponent Coalescence

In this chapter, as a first step, we aim to generalise the coalescence process when we have objects with more than one property. Secondly, we will analyse the Smoluchowki's system with a generalised multiplicative kernel and, lastly, we will map it to the multidimensional Burgers' equation.
Throughout this chapter, we will interchangeably use the notations to indicate the respective partial derivatives.

$$\frac{\partial}{\partial u}G = \partial_u G = G_u \,.$$

The natural naming scheme that was used in the previous chapter, where the name of the object is also the value of its property must now be broken. We will indicate objects as vectors $\mathbf{x} = (x_1, x_2, \ldots, x_d)$, where each component is the value for one property. Also in this case we are implicitly assuming that the properties are non-negative integer values. In particular, for the remainder of the manuscript, we will define $\mathbb{N}_0 := \{0, 1, 2, \ldots\}$ and use it as the set of property values. However, a remark must be made. We need to specify that in this setting the density $w_{\mathbf{0}}$ does not make sense, as the $\mathbf{0}$-object is an object with no properties. Differently from the one-dimensional case, however, we need properties of value 0, to allow for objects which have only some non-zero entries. Therefore, to avoid cumbersome notations, we will simply work with $\mathbf{x} \in \mathbb{N}_0^d$, knowing that we are implicitly excluding the zero-vector $\mathbf{0}$ from the calculations. Alternatively we can define $w_{\mathbf{0}}(t) = 0 \, \forall t$.

The first step will consist of generalising the Smoluchowski's equations into vector-form. Therefore, we will initially show some calculations in two dimensions for notational ease. We will then consider a coalescence process of the form:

$$\{\mathbf{x}, \mathbf{y}\} \to \{\mathbf{x} + \mathbf{y}\} \,,$$

where $\mathbf{x} = (x_1, \ldots, x_d)$ and $\mathbf{y} = (y_1, \ldots, y_d)$.

We indicate with $w_{\mathbf{x}}(t) = w_{x_1,\ldots,x_d}(t)$ the density of objects of type $\mathbf{x}$ at time t. By objects of type $\mathbf{x}$ we mean objects with d properties valued exactly x_i respectively

for each $i \in \{1, \dots, d\}$. We are still interested in the multiplicative coalescence and a first attempt at generalising the kernel would be

$$K(\mathbf{x}, \mathbf{y}) = \mathbf{x} \cdot \mathbf{y} \qquad .$$

Like before it is easy to see that this process is commutative as well. And similarly to the one-dimensional case, we have that the number of coagulations at every instant is given by

$$\frac{1}{2} w_{\mathbf{x}}(t) w_{\mathbf{y}}(t) K(\mathbf{x}, \mathbf{y}) \,,$$

where this time the coagulation kernel is between two vectors.

Let us proceed by considering the two-component case, bearing in mind that derivations for the N-component case are analogous. In the next chapter we will use a more generic notation, while here we show the single interactions between the various elements.

We can then obtain the Smoluchowski's equations in the two-dimensional case by describing the dynamics of the rate of change as

$$\dot{w}_{r,s}(t) = \{\text{all coagulations that generate } (r,s)\} - \{\text{all coagulations involving } (r,s)\} \,,$$

which translates to

$$\dot{w}_{r,s}(t) = \frac{1}{2} \sum_{x_1+y_1=r} \sum_{x_2+y_2=s} w_{x_1x_2} w_{y_1y_2} K(\mathbf{x}, \mathbf{y}) - \sum_{x_1,x_2 \in \mathbb{N}_0} K((r,s),(x_1,x_2)) w_{rs} w_{x_1x_2} \,.$$

By using the ansatz that $K(\mathbf{x}, \mathbf{y}) = \mathbf{x} \cdot \mathbf{y}$ we then have

$$\dot{w}_{r,s}(t) = \frac{1}{2} \sum_{x_1+y_1=r} \sum_{x_2+y_2=s} w_{x_1x_2} w_{y_1y_2} (x_1y_1 + x_2y_2) - \sum_{x_1,x_2 \in \mathbb{N}_0} w_{rs} w_{x_1x_2} (rx_1 + sx_2) \,,$$

we expand the both terms, and separate the second term into independent sums.

$$\begin{aligned} \dot{w}_{r,s}(t) = \frac{1}{2} \left[\sum_{\substack{x_1+y_1=r \\ x_2+y_2=s}} x_1y_1 w_{x_1x_2} w_{y_1y_2} + \sum_{\substack{x_1+y_1=r \\ x_2+y_2=s}} x_2y_2 w_{x_1x_2} w_{y_1y_2} \right] \\ - w_{rs} \left(r \sum_{x_1 \in \mathbb{N}_0} x_1 w_{x_1\cdot} + s \sum_{x_2 \in \mathbb{N}_0} x_2 w_{\cdot x_2} \right) \,, \end{aligned} \tag{3.1}$$

where we introduced the notation $w_{x\cdot}$ (or $w_{\cdot y}$) to indicate the partial sum over one parameter $w_{x\cdot} = \sum_y w_{xy}$ (or $w_{\cdot y} = \sum_x w_{xy}$).
We still use the generating function approach and we define the two parameters generating function

$$G(u, v, t) = \sum_{r,s \in \mathbb{N}_0} w_{rs}(t) e^{-ru-sv} \,,$$

where $w_{rs}(t)$ are solutions to the system (3.1). We now state a central theorem

Theorem 3.0.1. *Define $U := -\nabla G$, solutions to the system (3.1) before a time $t < t_c$ are also solutions to*

$$\frac{\partial}{\partial t}U(u,v,t) = -\mathbf{J}_U(U - M)\,,$$

where $M(t) := -\nabla G(0,0,t)$ and $\mathbf{J}_U$ is the Jacobian matrix of U.

Here the mass $M(t) = (M_1(t), M_2(t))$ represents the mass vector of the whole system. $M_1(t)$ represents the total mass of the elements of type 1 and $M_2(t)$ represents the whole mass of the elements of type 2.

To prove this theorem we will need some technical lemmas first.

Lemma 3.0.2. *Let $G(u,v,t) = \sum_{r,s\in\mathbb{N}_0} w_{r,s}(t)e^{-ru-sv}$ where $w_{rs}(t)$ are solutions to (3.1). Then*

$$\frac{\partial}{\partial t}G(u,v,t) = \frac{1}{2}[\frac{\partial}{\partial u}G(u,v,t)^2 + \frac{\partial}{\partial v}G(u,v,t)^2] - \nabla G(u,v,t)\cdot\nabla G(0,0,t)\,.$$

Proof. We start with

$$\frac{\partial}{\partial t}G(u,v,t) = \sum_{r,s\in\mathbb{N}_0} \dot{w}_{rs}(t)e^{-ru-sv}\,.$$

Equation 3.1 can be split into 3 terms:

$$\mathbf{I} = \frac{1}{2}\sum_{x_1+y_1=r} x_1y_1 \sum_{x_2+y_2=s} w_{x_1x_2}w_{y_1y_2} \tag{3.2}$$

$$\mathbf{II} = \frac{1}{2}\sum_{x_2+y_2=s} x_2y_2 \sum_{x_1+y_1=r} w_{x_1x_2}w_{y_1y_2} \tag{3.3}$$

$$\mathbf{III} = w_{rs}\left(r\sum_{x_1\in\mathbb{N}_0} x_1w_{x_1\cdot} + s\sum_{x_2\in\mathbb{N}_0} x_2w_{\cdot x_2}\right) \tag{3.4}$$

therefore,

$$\frac{\partial}{\partial t}G(u,v,t) = \sum_{r,s\in\mathbb{N}_0}(\mathbf{I})e^{-ru-sv} + \sum_{r,s\in\mathbb{N}_0}(\mathbf{II})e^{-ru-sv} - \sum_{r,s\in\mathbb{N}_0}(\mathbf{III})e^{-ru-sv}\,.$$

We will then solve the tree terms independently define the auxiliary terms

$$\sigma_v(x) = \sum_{s\in\mathbb{N}_0} w_{xs}e^{-sv} \qquad \sigma_u(y) = \sum_{r\in\mathbb{N}_0} w_{ry}e^{-ru}\,,$$

then we can proceed with the first term

$$\begin{aligned}
\sum_{rs}(\mathbf{I})e^{-ru-sv} &= \frac{1}{2}\sum_{r\in\mathbb{N}_0}\sum_{x_1+y_1=r} x_1y_1e^{-ru}\sum_{s\in\mathbb{N}_0}\sum_{x_2+y_2=s} w_{x_1x_2}w_{y_1y_2}e^{-(x_2+y_2)v} && \textit{Cauchy product}\\
&= \frac{1}{2}\sum_{r\in\mathbb{N}_0}\sum_{x_1+y_1=r} x_1y_1e^{-ru}\sigma_v(x_1)\sigma_v(y_1) && \textit{Cauchy product}\\
&= \frac{1}{2}\left(\sum_{r\in\mathbb{N}_0} r\sigma_v(x_1)e^{-ru}\right)\left(\sum_{r\in\mathbb{N}_0} r\sigma_v(y_1)e^{-ru}\right)\\
&= \frac{1}{2}\left(\sum_{r,s\in\mathbb{N}_0} rw_{rs}e^{-ru-sv}\right)^2\\
&= \frac{1}{2}G_u^2\,.
\end{aligned}$$

In a completely symmetric way we find the second term

$$\begin{aligned}
\sum_{r,s\in\mathbb{N}_0}(\mathbf{II})e^{-ru-sv} &= \frac{1}{2}\sum_{s\in\mathbb{N}_0}\sum_{x_2+y_2=s} x_2y_2e^{-sv}\sigma_u(x_2)\sigma_u(y_2)\\
&= \frac{1}{2}\left(\sum_{s\in\mathbb{N}_0} s\sigma_u(s)e^{-sv}\right)^2\\
&= \frac{1}{2}G_v^2\,,
\end{aligned}$$

and lastly

$$\begin{aligned}
\sum_{r,s\in\mathbb{N}_0}(\mathbf{III})e^{-ru-sv} &= \sum_{r,s\in\mathbb{N}_0} rw_{rs}e^{-ru-sv}\sum_{x,y\in\mathbb{N}_0} xw_{xy} + \sum_{r,s\in\mathbb{N}_0} sw_{rs}e^{-ru-sv}\sum_{x,y\in\mathbb{N}_0} yw_{xy}\\
&= G_uG_u(0,0,t) + G_vG_v(0,0,t)\\
&= \nabla G\cdot\nabla G(0,0,t)\,,
\end{aligned}$$

which results in

$$\frac{\partial}{\partial t}G(u,v,t) = \frac{1}{2}\left[\frac{\partial}{\partial u}G^2(u,v,t) + \frac{\partial}{\partial v}G^2(u,v,t)\right] - \nabla G(u,v,t)\cdot\nabla G(0,0,t)\,.$$

□

Unlike the one-dimensional case we have two different moments to work with, so we define

$$H = -\frac{\partial}{\partial u}G = \sum_{r,s\in\mathbb{N}_0} rw_{rs}e^{-ru-sv} \qquad K = -\frac{\partial}{\partial v}G = \sum_{r,s\in\mathbb{N}_0} sw_{rs}e^{-ru-sv}\,.$$

We then have

$$\partial_u H = -\sum_{r,s\in\mathbb{N}_0} r^2 w_{rs} e^{-ru-sv} \qquad \partial_v H = -\sum_{r,s\in\mathbb{N}_0} rs w_{rs} e^{-ru-sv}$$
$$\partial_u K = -\sum_{r,s\in\mathbb{N}_0} rs w_{rs} e^{-ru-sv} \qquad \partial_v K = -\sum_{r,s\in\mathbb{N}_0} s^2 w_{rs} e^{-ru-sv}\,.$$

So clearly $\partial_v H = \partial_u K$.

Lemma 3.0.3. *Under the above assumptions we have*

$$\frac{\partial}{\partial t} H = -\nabla H \cdot (\nabla G - \nabla G(0,0))\,,$$
$$\frac{\partial}{\partial t} K = -\nabla K \cdot (\nabla G - \nabla G(0,0))\,.$$

Proof. We will only provide the calculations for $\partial_t H$, as the calculations for $\partial_t K$ are completely symmetric.

$$\frac{\partial}{\partial t} H = -\frac{\partial}{\partial t}(G_u) = \sum_{r,s\in\mathbb{N}_0} r\dot{w}_{rs} e^{-ru-sv}\,.$$

Similarly to the previous Lemma, we split the equations into tree smaller terms to work with

$$\frac{\partial}{\partial t} H = \sum_{r,s\in\mathbb{N}_0} r\,(\mathbf{I}) e^{-ru-sv} + \sum_{r,s\in\mathbb{N}_0} r\,(\mathbf{II}) e^{-ru-sv} - \sum_{r,s\in\mathbb{N}_0} r(\mathbf{III}) e^{-ru-sv}\,,$$

shortening the calculations a bit (and recycling σ_s and σ_r from the previous lemma)

$$\begin{aligned}
\sum_{rs} r\,(\mathbf{I}) e^{-ru-sv} &= \frac{1}{2}\sum_{r\in\mathbb{N}_0} r \sum_{x_1+y+1=r} x_1 y_1 e^{-ru}\sigma_s(x_1)\sigma_s(y_1) \\
&= \frac{1}{2}\sum_{r\in\mathbb{N}_0}\sum_{x_1+y_1=r} (x_1+y_1) x_1 y_1 \sigma_s(x_1)\sigma_s(y_1) e^{-(x_1+y_1)u} \\
&= \frac{1}{2}\sum_{r\in\mathbb{N}_0}\sum_{x_1+y_1=r} x_1^2 \sigma_s(x_1) e^{-x_1 u} y_1 \sigma_s(y_1) e^{-y_1 u} \\
&\qquad + \frac{1}{2}\sum_{r\in\mathbb{N}_0}\sum_{x_1+y_1=r} x_1 \sigma_s(x_1) e^{-x_1 u} y_1^2 \sigma_s(y_1) e^{-y_1 u} \\
&= \left[\left(\sum_{r,s\in\mathbb{N}_0} r^2 w_{rs} e^{-ru-sv}\right)\left(\sum_{r,s\in\mathbb{N}_0} r w_{rs} e^{-ru-sv}\right)\right] \\
&= G_{uu}(-G_u) = (-H_u)H\,.
\end{aligned}$$

and for the second term we will need the auxiliary functions (we will only use σ'_u since σ'_v will only appear in the calculations for K_t)

$$\sigma'_v(x) = \sum_{s\in\mathbb{N}_0} s w_{xs} e^{-sv} \qquad \sigma'_u(y) = \sum_{r\in\mathbb{N}_0} r w_{ry} e^{-ru}\,,$$

$$\begin{aligned}
\sum_{r,s\in\mathbb{N}_0} r\,(\mathbf{II}) e^{-ru-sv} &= \frac{1}{2}\sum_{s\in\mathbb{N}_0}\sum_{x_2+y_2=s} x_2y_2e^{-sv}\sum_{r\in\mathbb{N}_0} r\sum_{x_1+y_1=r} w_{x_1x_2}w_{y_1y_2}e^{-ru}\\
&= \frac{1}{2}\sum_{s\in\mathbb{N}_0}\sum_{x_2+y_2=s} x_2y_2e^{-sv}\sum_{r\in\mathbb{N}_0}\sum_{x_1+y_1=r} (x_1+y_1) w_{x_1x_2}w_{y_1y_2}e^{-ru}\\
&= \frac{1}{2}\sum_{s\in\mathbb{N}_0}\sum_{x_2+y_2=s} x_2y_2e^{-sv}\left[\sigma'_u(x_2)\sigma_u(y_2)+\sigma_u(x_2)\sigma'_u(y_2)\right]\\
&= \frac{1}{2}\sum_{s\in\mathbb{N}_0}\sum_{x_2+y_2=s} x_2\sigma'_u(x_2)e^{-x_2v}\, y_2\sigma_u(y_2)e^{-y_2v}\\
&\qquad + \frac{1}{2}\sum_{s\in\mathbb{N}_0}\sum_{x_2+y_2=s} x_2\sigma_u(x_2)e^{-x_2v}\, y_2\sigma'_u(y_2)e^{-y_2v}\\
&= \left(\sum_{r,s\in\mathbb{N}_0} rsw_{rs}e^{-ru-sv}\right)\left(\sum_{r,s\in\mathbb{N}_0} sw_{rs}e^{-ru-sv}\right)\\
&= (-H_v)(-G_v) = H_vG_v\,,
\end{aligned}$$

and lastly

$$\begin{aligned}
\sum_{r,s\in\mathbb{N}_0} r(\mathbf{III})e^{-ru-sv} &= \sum_{r,s\in\mathbb{N}_0} r^2w_{rs}\sum_{x,y\in\mathbb{N}_0} xw_{xy}e^{-ru-sv} + \sum_{r,s\in\mathbb{N}_0} rsw_{rs}\sum_{x,y\in\mathbb{N}_0} yw_{xy}e^{-ru-sv}\\
&= -H_u\sum_{x,y\in\mathbb{N}_0} xw_{xy} - H_v\sum_{x,y\in\mathbb{N}_0} yw_{xy}\\
&= \nabla H\cdot\nabla G(0,0,t)\,.
\end{aligned}$$

Therefore,

$$\frac{\partial}{\partial t}H = -H_uH + H_vG_v - \nabla H\cdot\nabla G(0,0,t) = -\nabla H\cdot(\nabla G - \nabla G(0,0,t))\,.$$

□

We can now prove Theorem 3.0.1.

Proof. We defined $U = -\nabla G = (H,K)^T$ then we have

$$U_u = -\frac{\partial}{\partial u}\nabla G = (-G_{uu}, -G_{vu}) = (H_u, H_v = K_u)\,,$$

$$U_v = -\frac{\partial}{\partial v}\nabla G = (-G_{uv}, -G_{vv}) = (K_u = H_v, K_v)\,.$$

With this new notation we obtain

$$\begin{aligned} U_t &= (H_t, K_t)^T \\ &= \begin{pmatrix} -\nabla H \cdot (U - M) \\ -\nabla K \cdot (U - M) \end{pmatrix}, \end{aligned}$$

expanding and rearranging the last term we have the result

$$U_t = -\mathbf{J}_U (U - M)\,.$$

□

One interesting property to notice is the fact that

$$M(t) = -\nabla G(0, 0, t) = U(0, 0, t)$$

and particularly that

$$\frac{\partial}{\partial t} M(t) = \frac{\partial}{\partial t} U(0, 0, t) = (H_t(0, 0, t), K_t(0, 0, t))^T = (0, 0)^T\,,$$

therefore the total mass of the system, is again invariant with time. We will see in the next sections how to compute the critical time t_c. But first, let us take a detour in which we generalise the results obtained in this section to more generic bilinear kernels and generic dimensions d.

3.1 Generalising the Multiplicative Kernel

We've seen above a discussion about a multidimensional coalescence process, where we had a multiplicative kernel of $K(\mathbf{x}, \mathbf{y}) = \mathbf{x} \cdot \mathbf{y}$. The dot product involved there is a particular bilinear form $\mathbf{x} \cdot \mathbf{y} = \mathbf{x}^T I \mathbf{y}$. When we look at this through the lenses of our process we see that the dot product induces only symmetric diagonal matchings between elements of the same type. If we want a more generic pairing process we can generalise the multiplicative kernel to be

$$K_A(\mathbf{x}, \mathbf{y}) = \mathbf{x}^T A \mathbf{y}\,,$$

with A being a matrix of the proper dimensions and non-negative entries. In this case the previous case is simply a particular configuration of this more general system:

$$K(\mathbf{x}, \mathbf{y}) = K_I(\mathbf{x}, \mathbf{y})\,.$$

It is important to notice that if we want to preserve the commutativity of the Kernel, that is,

$$K_A(\mathbf{x}, \mathbf{y}) = K_A(\mathbf{y}, \mathbf{x})\,,$$

we must have that A is a symmetric matrix, this can be seen from

$$\begin{aligned} K_A(\mathbf{y}, \mathbf{x}) &= \mathbf{y}^T A \mathbf{x} \\ &= (\mathbf{x}^T A^T \mathbf{y})^T \\ &= \mathbf{x}^T A^T \mathbf{y} \\ &= K_{A^T}(\mathbf{x}, \mathbf{y})\,. \end{aligned}$$

Remark. We can assume symmetry in the matrix without loss of generality. Indeed, if we have an asymmetric matrix A, then

$$\begin{aligned} w_{\mathbf{x}} w_{\mathbf{y}} K_A(\mathbf{x}, \mathbf{y}) + w_{\mathbf{y}} w_{\mathbf{x}} K_A(\mathbf{y}, \mathbf{x}) \\ = w_{\mathbf{x}} w_{\mathbf{y}} K_{(A+A^T)}(\mathbf{x}, \mathbf{y})\,. \end{aligned}$$

Therefore, if we define a new kernel $A' = \frac{A+A^T}{2}$ we will obtain a symmetric kernel with the same dynamics of the asymmetric one.

As a result of this observation, we will assume symmetric matrices throughout. In our setting, since the model only allows for two different elements to join in a single aggregation event, we will have that all the ratio of coalescence will be positive, or at most zero. That translates to all the entries of the A matrix to be non-negative since the entries a_{ij} represents the rates at which objects of type i join with objects of type j. Since we are also assuming that the properties of the objects are always non-negative, it is trivial to show that $K_A(\mathbf{x}, \mathbf{y})$ is always non-negative.

If we start again, now the number of coagulations between two objects $\mathbf{x}, \mathbf{y}$ becomes

$$\frac{1}{2} w_{\mathbf{x}} w_{\mathbf{y}} \mathbf{x}^T A \mathbf{y}\,.$$

Let us introduce the region

$$\Omega_{\mathbf{k}} := \{\mathbf{x} \in \mathbb{N}_0^d \setminus \mathbf{k} : x_i \leq k_i \ \forall i\} \quad \forall \mathbf{k} \in \mathbb{N}_0^d \,.$$

which gathers the elements that satisfy $\mathbf{x} + \mathbf{y} = \mathbf{k}$. In particular, if we take $\mathbf{x} \in \Omega_{\mathbf{k}}$ then $(\mathbf{k} - \mathbf{x}) \in \Omega_{\mathbf{k}}$. With this the Smoluchowski's equations become

$$\begin{aligned} \dot{w}_{\mathbf{k}} &= \frac{1}{2} \sum_{\substack{\mathbf{x},\mathbf{y} \in \Omega_{\mathbf{k}} \\ \mathbf{x}+\mathbf{y}=\mathbf{k}}} w_{\mathbf{x}} w_{\mathbf{y}} \mathbf{x}^T A \mathbf{y} - \sum_{\mathbf{x} \in \mathbb{N}_0^d} w_{\mathbf{x}} w_{\mathbf{k}} \mathbf{x}^T A \mathbf{k} \\ &= \frac{1}{2} \sum_{\substack{\mathbf{x},\mathbf{y} \in \Omega_{\mathbf{k}} \\ \mathbf{x}+\mathbf{y}=\mathbf{k}}} w_{\mathbf{x}} w_{\mathbf{y}} \langle \mathbf{x}, \mathbf{y} \rangle_A - \sum_{\mathbf{x} \in \mathbb{N}_0^d} w_{\mathbf{x}} w_{\mathbf{k}} \langle \mathbf{x}, \mathbf{k} \rangle_A \,, \end{aligned} \tag{3.5}$$

where we introduce $\langle \mathbf{x}, \mathbf{y} \rangle_A = \langle \mathbf{x}, A\mathbf{y} \rangle = \langle A\mathbf{x}, \mathbf{y} \rangle$ with a slight abuse of notation, since A is not necessarily positive-definite in $\mathbb{R}^d$. Although we can say that if $a_{ii} \neq 0 \, \forall \, i$

$$0 = \mathbf{x}^T A \mathbf{x} \quad \text{Assume } \mathbf{x} \neq 0 \Rightarrow \exists j : x_j > 0 \Rightarrow 0 = \sum_{i,j} a_{i,j} x_i x_j \geq a_{jj} x_j^2 > 0 \lightning \,,$$

and if $a_{ii} = 0$ for some i then $\mathbf{x}^T A \mathbf{x} = 0 \Leftrightarrow x_i = 0$
Before moving on to the next step, we need to define the generating function

$$G(\mathbf{z}, t) = \sum_{\mathbf{k} \in \mathbb{N}_0^d} w_{\mathbf{k}} e^{-\mathbf{k}^T \mathbf{z}} \qquad \mathbf{z} \in \mathbb{C}^d \,,$$

where $w_{\mathbf{k}}(t)$ are solution to the system (3.5) before the gelation time t_c. We state an evolution of the Theorem 3.0.1

Theorem 3.1.1. *Let $U := -\nabla G$ where G is defined as above. Then, solutions to the system (3.5) with kernel defined by a matrix A with non-negative entries and for $t < t_c$, are also solutions to*

$$U_t = -\mathbf{J}_U A (U - M) \,,$$

where $M(t) := -\nabla G(\mathbf{0}, t)$ and $\mathbf{J}_U$ is the Jacobian matrix of U.

Proof. we have that

$$\nabla G(\mathbf{z}, t) = \sum_{\mathbf{k} \in \mathbb{N}_0^d} w_{\mathbf{k}} e^{-\mathbf{k}^T \mathbf{z}} \nabla(-\mathbf{k}^T \mathbf{z}) = -\sum_{\mathbf{k} \in \mathbb{N}_0^d} w_{\mathbf{k}} \mathbf{k} e^{-\mathbf{k}^T \mathbf{z}}$$

and more importantly:

$$\frac{\partial}{\partial t} G(\mathbf{z}, t) = \underbrace{\frac{1}{2} \sum_{\mathbf{k} \in \mathbb{N}_0^d} \sum_{\mathbf{y} \in \Omega_{\mathbf{k}}} w_{\mathbf{k}-\mathbf{y}} w_{\mathbf{y}} \langle \mathbf{k} - \mathbf{y}, \mathbf{y} \rangle_A e^{-\mathbf{k}^T \mathbf{z}}}_{\mathrm{I}} - \underbrace{\sum_{\mathbf{k} \in \mathbb{N}_0^d} \sum_{\mathbf{x} \in \mathbb{N}_0^d} w_{\mathbf{x}} w_{\mathbf{k}} \langle \mathbf{x}, \mathbf{k} \rangle_A e^{-\mathbf{k}^T \mathbf{z}}}_{\mathrm{II}}$$

with

$$\begin{aligned}
\mathbf{I} &= \frac{1}{2}\sum_{\mathbf{k}\in\mathbb{N}_0^d}\sum_{\mathbf{y}\in\Omega_\mathbf{k}} w_{\mathbf{k}-\mathbf{y}}w_\mathbf{y}\langle \mathbf{k}-\mathbf{y},\mathbf{y}\rangle_A e^{-\mathbf{k}^T\mathbf{z}} \\
&= \frac{1}{2}\sum_{\mathbf{k}\in\mathbb{N}_0^d}\sum_{\mathbf{y}\in\Omega_\mathbf{k}} \langle w_{\mathbf{k}-\mathbf{y}}(\mathbf{k}-\mathbf{y})e^{-(\mathbf{k}-\mathbf{y})^T\mathbf{z}}, w_\mathbf{y}\mathbf{y}e^{-\mathbf{y}^T\mathbf{z}}\rangle_A \\
&= \frac{1}{2}\sum_{\mathbf{y}\in\mathbb{N}_0^d}\sum_{\mathbf{k}\in\Omega_\mathbf{y}^c} \langle w_{\mathbf{k}-\mathbf{y}}(\mathbf{k}-\mathbf{y})e^{-(\mathbf{k}-\mathbf{y})^T\mathbf{z}}, w_\mathbf{y}\mathbf{y}e^{-\mathbf{y}^T\mathbf{z}}\rangle_A \\
&= \frac{1}{2}\sum_{\mathbf{y}\in\mathbb{N}_0^d}\sum_{\mathbf{x}\in\mathbb{N}_0^d} \langle w_\mathbf{x}\mathbf{x}e^{-\mathbf{x}^T\mathbf{z}}, w_\mathbf{y}\mathbf{y}e^{-\mathbf{y}^T\mathbf{z}}\rangle_A \\
&= \frac{1}{2}\sum_{\mathbf{y}\in\mathbb{N}_0^d}\langle \sum_{\mathbf{x}\in\mathbb{N}_0^d} w_\mathbf{x}\mathbf{x}e^{-\mathbf{x}^T\mathbf{z}}, w_\mathbf{y}\mathbf{y}e^{-\mathbf{y}^T\mathbf{z}}\rangle_A \\
&= \frac{1}{2}\langle \sum_{\mathbf{x}\in\mathbb{N}_0^d} w_\mathbf{x}\mathbf{x}e^{-\mathbf{x}^T\mathbf{z}}, \sum_{\mathbf{y}\in\mathbb{N}_0^d} w_\mathbf{y}\mathbf{y}e^{-\mathbf{y}^T\mathbf{z}}\rangle_A \\
&= \frac{1}{2}\langle \nabla G(\mathbf{z},t), \nabla G(\mathbf{z},t)\rangle_A \,,
\end{aligned}$$

while

$$\begin{aligned}
\mathbf{II} &= \sum_{\mathbf{k}\in\mathbb{N}_0^d}\sum_{\mathbf{x}\in\mathbb{N}_0^d} w_\mathbf{x}w_\mathbf{k}\langle \mathbf{x},\mathbf{k}\rangle_A e^{-\mathbf{k}^T\mathbf{z}} \\
&= \sum_{\mathbf{k}\in\mathbb{N}_0^d} w_\mathbf{k}\langle \sum_{\mathbf{x}\in\mathbb{N}_0^d} w_\mathbf{x}\mathbf{x},\mathbf{k}\rangle_A e^{-\mathbf{k}^T\mathbf{z}} \\
&= \langle \sum_{\mathbf{x}\in\mathbb{N}_0^d} w_\mathbf{x}\mathbf{x}, \sum_{\mathbf{k}\in\mathbb{N}_0^d} w_\mathbf{k}\mathbf{k}e^{-\mathbf{k}^T\mathbf{z}}\rangle_A \,.
\end{aligned}$$

Recall that we call $M = -\nabla G(\mathbf{0},t)$ which is the total mass of the system, therefore we have

$$\mathbf{II} = -\langle M, \nabla G(\mathbf{z},t)\rangle_A$$

and therefore

$$G_t(\mathbf{z},t) = \frac{1}{2}\langle \nabla G(\mathbf{z},t), \nabla G(\mathbf{z},t)\rangle_A + \langle M, \nabla G(\mathbf{z},t)\rangle_A \,.$$

We defined

$$U(\mathbf{z},t) = -\nabla G(\mathbf{z},t) = -(\partial_1 G, \partial_2 G, \dots)\,,$$

where

$$\partial_i G(\mathbf{z},t) = -\sum_{k\in\mathbb{N}_0^d} w_k(t)k_i e^{-\mathbf{k}^T\mathbf{z}}$$

are scalar valued functions. We call

$$U_i(\mathbf{z},t) = -\partial_i G(\mathbf{z},t)$$

and define

$$[DF] = (\partial_1 F, \partial_2 F, \dots)^T$$

as the derivative in the numerator layout convention. We want to find

$$\begin{aligned}\frac{\partial}{\partial t}U &= -(\partial_t\partial_1 G, \partial_t\partial_2 G, \dots)^T \\ &= -(\partial_1\partial_t G, \partial_2\partial_t G, \dots)^T = -\nabla G_t = -[DG_t]^T\,. \end{aligned} \tag{3.6}$$

We then have that

$$[DG_t] = \frac{1}{2}[D\langle \nabla G, \nabla G\rangle_A] + [D\langle M, \nabla G\rangle_A] = \frac{1}{2}[D\langle U, U\rangle_A] - [D\langle M, U\rangle_A]\,.$$

We have

$$[D\langle \mathbf{x}, \mathbf{x}\rangle_A] = 2\mathbf{x}^T A \quad \text{and} \quad [D\langle M, \mathbf{x}\rangle_A] = M^T A\,.$$

By means of the chain rule we then obtain that

$$\begin{aligned}[DG_t] &= \frac{1}{2}[D\langle U, U\rangle_A]\mathbf{J}_U - M^T A\mathbf{J}_U \\ &= U^T A\mathbf{J}_U - M^T A\mathbf{J}_U \\ &= (U^T - M^T)A\mathbf{J}_U\,,\end{aligned}$$

therefore, by (3.6)

$$\frac{\partial}{\partial t}U = -[DG_t]^T = -(A\mathbf{J}_U)^T(U - M)\,,$$

but $\mathbf{J}_U$ is the Hessian matrix of G, and therefore symmetric, so

$$\frac{\partial}{\partial t}U = -\mathbf{J}_U A(U - M)\,.$$

Remark. $D_{ij}G = \sum_{\mathbf{k}} w_{\mathbf{k}} k_i k_j e^{-\mathbf{k}^T\mathbf{z}} = D_{ji}G$.

□

We then retain the nice parallelism that solutions to the Smoluchowski's system of equations with a multiplicative kernel, as we proposed, are also solutions to the multidimensional inviscid Burgers' equation.

In both Theorems, we specify that the solutions hold only before the critical time for the coalescence process. We set now to find a formula for it.

3.1.1 Blow up time

In the one-dimensional case we had that for the monodisperse initial conditions the critical time is $t_c = 1$ and it was obtained through solving the one-dimensional Burgers' equation directly, corresponding to the solution developing a discontinuity. In another fashion, the blow up time for the monocomponent Smoluchowski's equations can be computed through the second moment:

$$m_2(t) = \sum_{x \in \mathbb{N}_0} x^2 w_x(t)\,.$$

Noticing that when two particles joined together with the process $\{x, y\} \to x + y$ the increase in the squared mass sum would be just $2xy$ so

$$\frac{dm_2}{dt} = \sum_{x,y \in \mathbb{N}_0} xyK(x,y) w_x(t) w_y(t) = \sum_{x,y \in \mathbb{N}_0} x^2 y^2 w_x(t) w_y(t) = (m_2(t))^2\,,$$

which can be solved by means of separation of variables and obtain

$$m_2(t) = \frac{1}{c - t}\,,$$

where $c = 1/m_2(0)$ which for the monodisperse initial conditions we clearly have $c = 1$, giving us the expected $t_c = 1$. In our more general case we will define the moment-generating function

$$M_{\mathbf{k}}(\mathbf{z}) = \mathbb{E}\left[e^{\langle \mathbf{k}, \mathbf{z} \rangle}\right]$$

and we will define the nth moment as $M^{(n)} = [D^n_{\mathbf{z}} M_{\mathbf{k}}(\mathbf{z})]_{|\mathbf{z}=0}$ therefore having

$$[D_{\mathbf{z}} M_{\mathbf{k}}(\mathbf{z})] = \mathbb{E}(\mathbf{k}^T e^{\langle \mathbf{k}, \mathbf{z} \rangle})$$

and therefore

$$\begin{aligned}
M^{(2)}(t) = [D^2_{\mathbf{z}} M_{\mathbf{k}}(\mathbf{z})] &= [D_{\mathbf{z}}[D_{\mathbf{z}} M_{\mathbf{k}}(\mathbf{z})]] \\
&= \mathbb{E}\left(\left[D_{\mathbf{z}} \mathbf{k}^T e^{\langle \mathbf{k}, \mathbf{z} \rangle}\right]\right) \\
&= \mathbb{E}\left(\begin{bmatrix} k_1 D_1 e^{\langle \mathbf{k}, \mathbf{z} \rangle} & k_1 D_2 e^{\langle \mathbf{k}, \mathbf{z} \rangle} \dots \\ k_2 D_1 e^{\langle \mathbf{k}, \mathbf{z} \rangle} & k_2 D_2 e^{\langle \mathbf{k}, \mathbf{z} \rangle} \dots \\ \vdots & \ddots \end{bmatrix}\right) \\
&= \mathbb{E}\left(\begin{bmatrix} k_1 \mathbf{k}^T \\ k_2 \mathbf{k}^T \\ \vdots \end{bmatrix} e^{\langle \mathbf{k}, \mathbf{z} \rangle}\right) \\
&= \mathbb{E}(\mathbf{k}\mathbf{k}^T e^{\langle \mathbf{k}, \mathbf{z} \rangle})\,.
\end{aligned}$$

Thus,

$$M^{(2)}(t) = [D^2_{\mathbf{z}} M_{\mathbf{k}}(\mathbf{z})]_{|\mathbf{z}=0} = \mathbb{E}\left(\mathbf{k}\mathbf{k}^T\right) = \sum_{\mathbf{k}\in\mathbb{N}_0^d} \mathbf{k}\mathbf{k}^T w_{\mathbf{k}}(t)\,.$$

We can then prove

Theorem 3.1.2. *In a multicomponent coalescence process with multiplicative kernel $K_A(\mathbf{x},\mathbf{y})$ for some symmetric matrix with non-negative entries A, given by Equation (3.5), the gelation time is given by the smallest t such that*

$$\det(C - At) = 0\,,$$

where $C^{-1} = M^{(2)}(0)$

Proof. similarly to the one-dimensional case, when we have a coagulation event where $\{\mathbf{k},\mathbf{h}\} \to \{\mathbf{k}+\mathbf{h}\}$, the change in the second moment will be, given that

$$(\mathbf{k}+\mathbf{h})(\mathbf{k}^T+\mathbf{h}^T) = \mathbf{k}\mathbf{k}^T + \mathbf{h}\mathbf{k}^T + \mathbf{k}\mathbf{h}^T + \mathbf{h}\mathbf{h}^T\,,$$

and recalling that we are assuming A symmetric,

$$\begin{aligned}
\frac{dM^{(2)}(t)}{dt} &= \frac{1}{2}\sum_{\mathbf{k},\mathbf{h}\in\mathbb{N}_0^d} (\mathbf{k}\mathbf{h}^T + \mathbf{h}\mathbf{k}^T) w_{\mathbf{k}}(t) w_{\mathbf{h}}(t) K(\mathbf{k},\mathbf{h}) \\
&= \frac{1}{2}\sum_{\mathbf{k},\mathbf{h}\in\mathbb{N}_0^d} (\mathbf{k}\mathbf{h}^T + \mathbf{h}\mathbf{k}^T) w_{\mathbf{k}}(t) w_{\mathbf{h}}(t) (\mathbf{k}^T A\mathbf{h}) \\
&= \frac{1}{2}\sum_{\mathbf{k},\mathbf{h}\in\mathbb{N}_0^d} w_{\mathbf{k}}(t) w_{\mathbf{h}}(t) \mathbf{k}(\mathbf{k}^T A\mathbf{h})\mathbf{h}^T + \frac{1}{2}\sum_{\mathbf{k},\mathbf{h}\in\mathbb{N}_0^d} w_{\mathbf{k}}(t) w_{\mathbf{h}}(t) \mathbf{h}(\mathbf{h}^T A\mathbf{k})\mathbf{k}^T \\
&= \frac{1}{2}\sum_{\mathbf{k},\mathbf{h}\in\mathbb{N}_0^d} w_{\mathbf{k}}(t)\mathbf{k}\mathbf{k}^T A w_{\mathbf{h}}(t)\mathbf{h}\mathbf{h}^T + \frac{1}{2}\sum_{\mathbf{k},\mathbf{h}\in\mathbb{N}_0^d} w_{\mathbf{h}}(t)\mathbf{h}\mathbf{h}^T A w_{\mathbf{k}}(t)\mathbf{k}\mathbf{k}^T \\
&= \frac{1}{2}\left(\sum_{\mathbf{k}\in\mathbb{N}_0^d} w_{\mathbf{k}}(t)\mathbf{k}\mathbf{k}^T\right) A \left(\sum_{\mathbf{h}\in\mathbb{N}_0^d} w_{\mathbf{h}}(t)\mathbf{h}\mathbf{h}^T\right) \\
&\qquad + \frac{1}{2}\left[\left(\sum_{\mathbf{k}\in\mathbb{N}_0^d} w_{\mathbf{k}}(t)\mathbf{k}\mathbf{k}^T\right) A \left(\sum_{\mathbf{h}\in\mathbb{N}_0^d} w_{\mathbf{h}}(t)\mathbf{h}\mathbf{h}^T\right)\right]^T\,,
\end{aligned}$$

but $M^{(2)}(t)$ is symmetric, as well as A, so in the end we obtain

$$\frac{dM^{(2)}(t)}{dt} = A\left(M^{(2)}(t)\right)^2\,,$$

which is a separable differential equation with solution

$$M^{(2)}(t) = (C - At)^{-1}\,,$$

where C is such that $C^{-1} = M^{(2)}(0)$ which is a constant that depends on the initial distribution.

□

In this multidimensional scenario the initial conditions change a little. For example, the monodisperse initial conditions for a d-coloured system, now asks that the only types of molecule present in the solution at the beginning are those of the form $e_i,\ i \in [d]$, that is,

$$e_1 = (1, 0, \ldots, 0), \quad e_2 = (0, 1, \ldots, 0), \quad \ldots, \quad e_d = (0, \ldots, 0, 1)\,.$$

This means that the only non-zero densities are $w_{e_i}(0) = 1$ since we are normalising them by M_i respectively. This means that the $w_{\mathbf{x}}(t)$ represents the distribution of objects of a certain type in the system, respect to which mass we decide to normalise by.

Corollary 3.1.3. *With monodisperse initial conditions as described above we have that the blow up time to the process described in Theorem 3.1.2 is*

$$t_c = \frac{1}{\|A\|}\,.$$

Proof. In this setting, applying Theorem 3.1.2, we obtain $C = I$ and therefore the critical time is given by $\det(I - At) = 0$. If we recognise the characteristic equation $\det(\lambda I - A)$ for the eigenvalues of the matrix A, where in this case $\lambda = \frac{1}{t}$, the smallest time at which we have a blow up is the one relative to the biggest eigenvalue of A. □

It is also worth noting that as it is mentioned in the Aldous [Ald99], in general, the multiplication kernel, is of course homogeneous and $K(cx, cy) = c^{\gamma}K(x, y)$. But in particular for the multiplication kernel $\gamma = 2$. It can be shown that we are exactly at the boundary of instant gelation. That is, we have that $t_c < \infty$ if $\gamma > 1$ and $t_c = 0$ for $\gamma > 2$.

Chapter 4

Multicoloured Random Graphs

We saw how the Smoluchowski's equations generalise quite well in higher dimensions. We attempt to obtain the same random graph approach we saw in the one-dimensional case, also for higher dimensions.
As a general setting we will have elements of various types involved in the coagulations that will be represented in the random graph language by multicoloured nodes. These nodes will then create links between them at different rates as described by the aggregating kernel.
We will show the approach for the case of a two-dimensional coalescence between two types of nodes, *black* and *red*, for simplicity and not to bog down too much the argument with notation. For now, the edges joining these two types of node are not typed themselves but we will see how to give the edges a colour as well.

4.1 Degree Distribution

In our discussion, we do not have a specific degree distribution describing a specific process a priori, but instead, we derive it for a given aggregation kernel and its rates. Indeed, one of the main reasons why we stick to monodisperse initial conditions, is that the degree distribution is defined by a process that starts with an edgeless graph in which we randomly add edges. It is not clear how starting the process from a different initial condition would influence the evolution of the degree distribution.

The degree distribution is a local property that depends solely on a node and its immediate neighbours. Given that we depend on the aggregation rates, that act on specific types of nodes, we cannot give a degree distribution for the whole system directly, but instead, we can construct a degree distribution for each type of node and afterwards, build a system-wide degree distribution as a weighted mean. For example, suppose that we pick a black node, and look at its neighbours, the degree distribution tells us how likely it is to have b black neighbours and r red neighbours, with the number $u_B(b, r)$.

We work in a time dependent setting where the longer we wait the more our system will create new connections, and with it, the degree distribution will change.

In particular, the dynamics in time of the distribution $u_B(b,r)$ are influenced by all the new connections, that is

$$\frac{du_B(b,r)}{dt} = a_{BB}u_B(b-1,r) + a_{BR}u_B(b,r-1) - (a_{BB}+a_{BR})u_B(b,r)\,. \tag{4.1}$$

This equation represents reaching the state $u_B(b,r)$ by having already, either $b-1$ black connections and adding a new one, or $r-1$ red connections and add a new one, or departing from that particular state by creating a new connection to any new node. These dynamics are directed by the rates a_{ij}, which are the entries of the aggregation kernel. (i.e. a_{ij} indicates the rate at which we create a connection from a node of type i to a node of type j).

We define now the multivariate Generating Function for the degree distribution of a black node

$$U_B(x,y) = \sum_{b,r\in\mathbb{N}_0} u_B(b,r)x^b y^r\,.$$

Knowing that $[x^b y^r]xU_B(x,y) = u_B(b-1,r)$, and $[x^b y^r]yU_B(x,y) = u_B(b,r-1)$ we have that

$$\frac{dU_B(b,r)}{dt} = a_{BB}xU_B(x,y) + a_{BR}yU_B(x,y) - (a_{BB}+a_{BR})U_B(x,y) \tag{4.2}$$

$$= U_B(x,y)(-a_{BB}-a_{BR}+a_{BB}x+a_{BR}y)\,. \tag{4.3}$$

If we proceed similarly for red nodes and solve the corresponding ODEs, we obtain the degree distribution generating functions at a time t for both types of nodes

$$U_B(x,y,t) = e^{a_{BB}(x-1)t}e^{a_{BR}(y-1)t} \tag{4.4}$$

$$U_R(x,y,t) = e^{a_{RB}(x-1)t}e^{a_{RR}(y-1)t}\,. \tag{4.5}$$

Following the reasoning, the nodes in the random graph are selected uniformly at random, the generic degree distribution generating function is given by

$$U(x,y) = \eta_B U_B(x,y) + \eta_R U_R(x,y)\,, \tag{4.6}$$

where η_B, η_R are the distribution of types of nodes in the system. That is, $\sum_i \eta_i = 1$.

4.2 Connected Component Size

Another key component and ultimately, the focus of this discussion, is how big is a connected component. Recall the quantities of interest in this discussion $w_{\mathbf{k}}$, in our multidimensional case these are the distribution in time of $\mathbf{k}$-objects, that is multi component objects $(k_1, k_2, \ldots, k_d)$ that have k_1 atoms of type 1, k_2 atoms of type 2 and so on, or alternatively that are the sum of $k_i e_i = (0,\ldots,k_i,\ldots,0)$ multi-objects for all i. For example, in the two-dimensional case the trees in Figure 3.1, represent a particular $(3,3)$ particle. Now, if we select a node, chosen uniformly at random among all our nodes, depending on the distribution of types in the system (i.e. η_B and η_R in our two-dimensional example) it will be of a specific type.

Claim We have seen that the degree distribution for the nodes is Poisson in nature. We claim now that, similarly to the one-dimensional case, in the subcritical regime, the components of the graph with our Poisson distribution are locally tree-like with multicomponent Poisson offspring distribution.

Following the claim then, each node that we select will be part of a tree that can be viewed as a multi-typed branching process, with multidimensional Poisson offspring distribution, given by the degree distribution. Depending on the type of the selected node, if we interpret it as the root of the tree, the total progeny distribution of the branching process will vary. Therefore, it is natural to define two Generating Functions that generate the total progeny distribution of the branching processes that either start with a *Black* or *Red* node:

$$W_B(x,y) = \sum_{b,r\in\mathbb{N}_0} w_B(b,r)x^b y^r \qquad W_R(x,y) = \sum_{b,r\in\mathbb{N}_0} w_R(b,r)x^b y^r \,.$$

Similarly to how we did with the degree distribution, the total progeny distribution will be just a weighted mean

$$W(x,y) = \eta_B W_B(x,y) + \eta_R W_R(x,y)\,. \tag{4.7}$$

4.2.1 Weakly-connected components

In this discussion, we are mainly interested in the study of weakly connected components of a graph. In this scenario, weakly connected components tell us the total amount of atomic objects that make up a single entity, independent of its actual composition. For example, when studying weakly connected components, we don't distinguish a $(10,0)$-object (i.e. a component with only black nodes) from a $(5,5)$-object (i.e. half black and half red nodes in a component, in any configuration), since they both fall under the umbrella of a 10-object. Thus, effectively, studying weakly connected components projects a system that follows multidimensional dynamics onto a single dimension. We will use Generating Functions (specialised for the type of initial node i) defined as

$$W_i(z) = \sum_{n\in\mathbb{N}_0} w_i(n)z^n\,,$$

where

$$w_i(n) = \sum_{b+r=n} w_i(b,r) \quad b,r\in\mathbb{N}_0\,,$$

so effectively a convolution. If we notice that $x^b y^r|_{x=y} = z^{b+r}$, this is equivalent to saying

$$W_i(z) = W_i(z,z)\,.$$

4.3 Excess Distributions

The notion of excess distribution will be useful in the following sections. In Bergeron [BLL97], through the theory of combinatorial species of structure, we can find a handy generalisation to the concept of *excess distribution*.
In short, If we have a distribution $(g_n)_{n\in\mathbb{N}_0}$ generated by a Generating Function

$$G(z) = \sum_{n\in\mathbb{N}_0} g_n z^n \,,$$

the excess distribution (intuitively, what we refer to when speaking of "follow an edge and look at the resulting distribution of the neighbour reached") is associated with the formal derivative

$$D_z G(z) = \sum_{n\in\mathbb{N}_0} g'_n z^n = \sum_{n\in\mathbb{N}_0} (n+1) g_{n+1} z^n \,.$$

This concept can be extended into multiple dimensions using formal partial derivatives. But it is still not enough. Indeed, carrying on the one-dimensional example, the generating function $G'(z)$ requires to be normalised to be generating a distribution. One of the defining characteristics of a distribution is indeed that

$$\sum_{n\in\mathbb{N}_0} g_n = 1 \,,$$

but this translates on the generating function as

$$G(1) = 1 \,.$$

As of now, the quantity

$$D_z G(1) = \sum_{n\in\mathbb{N}_0} n g_n$$

represents the expectation (or first moment) of the distribution $(g_n)_n$.
We define the moments of a bivariate Generating function $G(x,y)$ as

$$\mu_{ij}(G) = \sum_{b,r\in\mathbb{N}_0} b^i r^j g(b,r) = \left[(x\frac{\partial}{\partial x})^i (y\frac{\partial}{\partial y})^j G(x,y) \right]_{|x=y=1} \,. \tag{4.8}$$

Then we define the excess distributions of the bivariate generating function $G(x,y)$ as

$$\partial_x G(x,y) = \frac{1}{\mu_{10}(G)} \frac{\partial G}{\partial x}(x,y) \qquad \partial_y G(x,y) = \frac{1}{\mu_{01}(G)} \frac{\partial G}{\partial y}(x,y) \,. \tag{4.9}$$

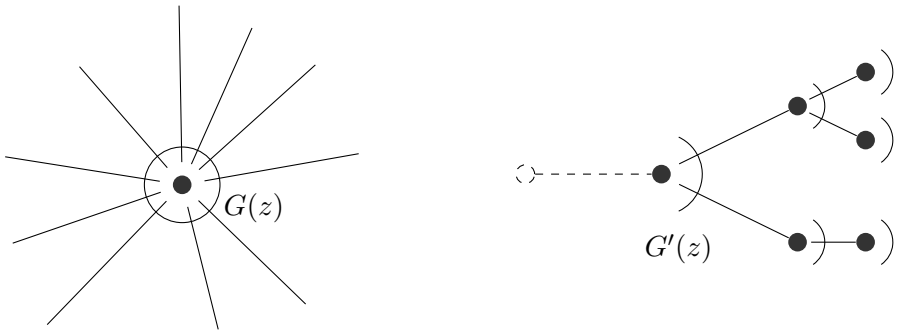

Figure 4.1: We schematically represent the degree distribution as a full circle around a node and the excess distribution as an half circle.

4.3.1 Excess degree

In the previous sections, we saw that we have a degree distribution dependent on the type of node we select. Assume we select a black node, its degree distribution will be generated by

$$U_B(x,y) = \sum_{b,r\in\mathbb{N}_0} u_B(b,r)x^b y^r \,.$$

The intuitive idea for the excess degree distribution in one dimension is selecting a random node and following one of its edges, and then look at the degree of the resulting neighbour. In the multidimensional case, we must be careful not only where we end up when we follow an edge, but also where we arrive from.

Propagating the edge colour A small parenthesis must be made on how we assign an edge its colour. We select a node, of a certain colour, as the root, then we looking at its neighbours. We propagate through all the undirected edges and turn them into a directed edge of the colour of the neighbour it reaches as shown in Figure 4.3. The colour and direction of an edge are only dependent on the chosen root node, if we select a different root node the direction and colour of an edge might change (see Figure 4.4). This is merely a way to get closer to the original meaning of degree distribution, which tells us that a node will have b black edges and r red edges, while in reality in this case it is telling us that a node is *connected* to b black nodes and r red nodes. Therefore, the conflicts of this relativistic interpretation do not affect the underlying system in any way.

Going back to our example, we already assumed that we chose initially a black node, which will have a certain distribution of black and red edges stemming from it. We choose an edge to follow and we land on another node, the degree distribution of the node we land on will influence the excess degree distribution of the node we started from. When we only have one type of node this difference gets flattened, but

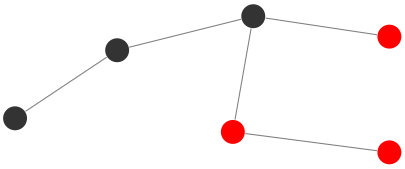

Figure 4.2: Base Graph

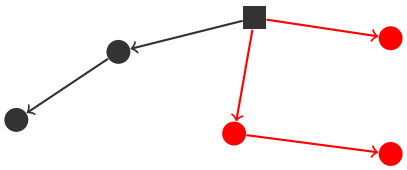

Figure 4.3: Select a node (square) and propagate the edge colour

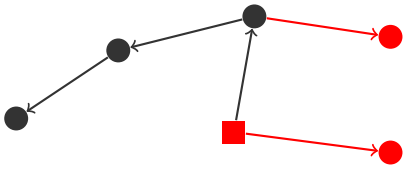

Figure 4.4: Follow an edge, the propagated colours change

in this case, our black node will have two different excess degree distributions.

$$u_B^B(b,r) = \frac{b+1}{\mu_{10}(U_B)} u_B(b+1,r) \qquad u_R^B(b,r) = \frac{b+1}{\mu_{10}(U_R)} u_R(b+1,r)\,, \tag{4.10}$$

generated by $U_B^B(x,y)$ and $U_R^B(x,y)$ respectively. We use the u_J^I notation to indicate the direction $I \to J$. We divide by the respective moments to make sure the distributions sum up to 1, as discussed in Section 4.3. Using the generating functional notation we just introduced, then

$$U_B^B(x,y) = \partial_x U_B(x,y) \qquad U_R^B(x,y) = \partial_x U_R(x,y)\,.$$

4.3.2 Excess size distribution

Albeit not as immediate as the excess degree distribution, the excess total progeny distribution is still rather intuitive. Copying the intuitive formulation for the excess degree, say we select a black node, and follow one of its edges to a red node. If we momentarily forget the initial black node, the red node we reached will be the root of a tree with a certain progeny distribution, therefore the excess progeny distribution is equivalent to the question "what is the total progeny distribution given that we have at least one black node in it?". In formulas, this results in defining the following distributions:

$$W_B^B(x,y) = \partial_x W_B(x,y) \qquad W_R^B(x,y) = \partial_x W_R(x,y)$$

$$W_B^R(x,y) = \partial_y W_B(x,y) \qquad W_R^R(x,y) = \partial_y W_R(x,y)\,.$$

4.4 Deriving the System

Let us return to the bi-dimensional case. We will now use an example to showcase the reasoning behind the derivations of the implicit algebraic equations that make up a system similar to the one used in the introduction. The formal justification behind this reasoning is very complex, and outside the scope of this manuscript, as it involves the whole theory of *combinatorial species of structures* [BLL97]. We will present some of the concepts of the theory digested and adapted to the context of interest, along with some pictures, that, hopefully, will provide enough intuitive justifications to the reader.

Before we begin, we shall give a brief overview of the very abstract concept of *structure*. In the most general sense, a structure $S = (\gamma, D)$ is a *construction* γ performed on a set of data D. A construction, in the broader sense, is a rule that is used to describe relations between the objects from the data set D. For example, an oriented cycle structure on the data $D = \{1, 2, 3, 4\}$ is defined by the construction $\gamma = \{(1, 2), (2, 3), (3, 4), (4, 1)\}$ of the edges.

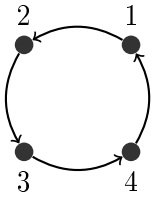

To bring this idea back in a more practical scenario, closer to our needs, then, on a set of nodes, a structure can be represented by a generating function U. For example, we can apply a "degree distribution U" construction to obtain a U-structure that describes a graph with a degree distribution defined by U. Given the incredibly general definitions, it shouldn't come as a surprise when we start to create structures of structures, or otherwise compose different structures through a set of operations, to create new ones.

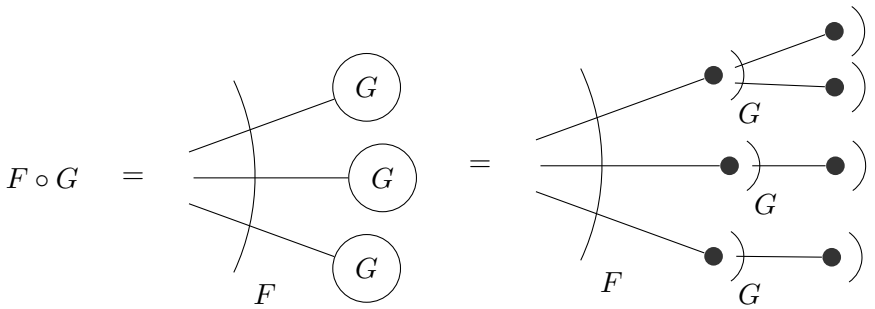

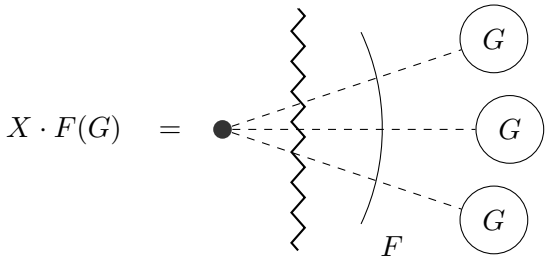

Let us choose a node uniformly at random, and for the sake of exposition, let us assume that we picked a black node. This node, will be part of a connected component with a certain composition of other black and red nodes, with distribution generated by $W_B(x, y)$. Select the node as the root of the tree-like component (as we assume from the claim), and propagate through all the edges of the component, as described in Section 4.3.1. The amount of edges and their type distribution is described by the degree distribution $U_B(x, y)$. The nodes at the end of each edge stemming from the initial black node, if we momentarily forget about the latter, can be seen as roots of other tree-like structures that they themselves will have a specific composition distribution generated by $W_i(x, y)$ depending on the type of the root we reached.

However, since they are connected to the initial black root, they will instead be the roots of rooted trees with the excess progeny distribution generated by $\partial_x W_i(x, y)$.

Theorem 4.4.1. *Let $W_B(x, y)$ and $W_R(x, y)$ be the generating functions generating the total progeny distribution of rooted trees of a bivariate Poisson process, starting with a black or red node respectively. And let $U_B(x, y), U_R(x, y)$ be the degree distributions of vertices of the respective type. Then, W_B and W_R are implicitly defined through the systems*

$$W_B(x, y) = x \cdot U_B\left[\partial_x W_B(x, y), \partial_x W_R(x, y)\right] \tag{4.11}$$
$$\partial_x W_B(x, y) = x \cdot \partial_x U_B\left[\partial_x W_B(x, y), \partial_x W_R(x, y)\right] \tag{4.12}$$
$$\partial_x W_R(x, y) = y \cdot \partial_x U_R\left[\partial_y W_B(x, y), \partial_y W_R(x, y)\right] \tag{4.13}$$

and

$$W_R(x, y) = y \cdot U_R\left[\partial_y W_B(x, y), \partial_y W_R(x, y)\right] \tag{4.14}$$
$$\partial_y W_B(x, y) = x \cdot \partial_y U_B\left[\partial_x W_B(x, y), \partial_x W_R(x, y)\right]$$
$$\partial_y W_R(x, y) = y \cdot \partial_y U_R\left[\partial_y W_B(x, y), \partial_y W_R(x, y)\right]$$

Proof. Equation (4.11) is derived through the discussion in the above paragraph (refer to Figure 4.5 for a visual example), and Equations (4.12) to (4.13) through a self-similarity argument. System (4.14) is completely symmetric. □

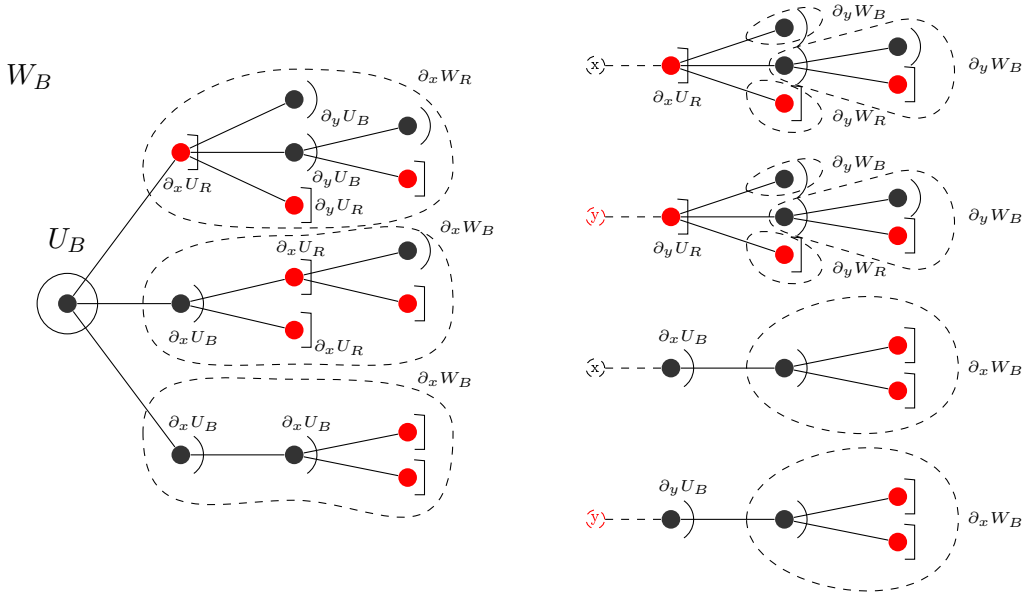

Figure 4.5: Schematic representations of a particular realisation for the system of implicit algebraic equations. On the left we have a visual justification to the formula (3.10), on the right we show examples for the excess distributions formulas.

4.5 Solving

We show two fundamental theorems that are needed to solve the system.

Theorem 4.5.1. *Every system of equations*

$$\begin{aligned} Y_1 &= H_1(X_1, \dots, X_n, Y_1, \dots, Y_k) \\ Y_2 &= H_2(X_1, \dots, X_n, Y_1, \dots, Y_k) \\ &\vdots \\ Y_k &= H_k(X_1, \dots, X_n, Y_1, \dots, Y_K) \end{aligned}$$

admits a solution $Y_1(X_1, \dots, X_n), \dots, Y_k(X_1, \dots, X_n)$ *unique up to isomorphism, whenever the following conditions for the species* $H_1, \dots, H_k$ *are satisfied:*

1. *for any* m, $1 \leq m \leq k$ $H_m(0, \dots, 0) = 0$,

2. *the Jacobian matrix* $\frac{\partial H_i}{\partial Y_j}(0, \dots, 0)$, $1 \leq i, j \leq k$ *is nilpotent.*

An important special case is given by the system

$$\begin{aligned} Y_1 &= X_1 R_1(Y_1, \dots, Y_k) \\ Y_2 &= X_2 R_2(Y_1, \dots, Y_k) \\ &\vdots \\ Y_k &= X_k R_k(Y_1, \dots, Y_k) \end{aligned}$$

which satisfies the conditions of Theorem 3.4.1. Therefore, for series $R_i(x_1, \dots, x_k)$ $i = 1, \dots, k$ in the ring $\mathbb{A}[x_1, \dots, x_k]$ of formal power series there exists a unique formal power series $A_i(x_1, \dots, x_k)$ that satisfies the system of equation

$$A_i(x_1, \dots, x_k) = x_i R_i(x_1, \dots, x_k) \qquad i = 1, \dots, k\,. \tag{4.15}$$

We can now state the Good-Lagrange Inversion Formulas Theorem (G-LIF)

Theorem 4.5.2. *Let* $\mathbf{R}(\mathbf{x}) = (R_1(\mathbf{x}), \dots, R_k(\mathbf{x}))$ *be a vector of formal power series in the variables* $\mathbf{x} = (x_1, \dots, x_k)$. *Let* $\mathbf{A}(\mathbf{x})$ *be a vector of formal power series in the variables* $\mathbf{x}$ *satisfying (4.15). Then, for any formal power series* $F(\mathbf{x})$ *and all* $\mathbf{n} \in \mathbb{N}_0^k$ *we have:*

$$[\mathbf{x}^\mathbf{n}] F\left[\mathbf{A}(\mathbf{x})\right] = [\mathbf{t}^\mathbf{n}]\, F(\mathbf{t}) \det K(\mathbf{t}) \mathbf{R}^\mathbf{n}(\mathbf{t})\,,$$

where $K(\mathbf{t})$ *has the entries defined as*

$$[K(t_1, \dots, t_k)]_{i,j} = \delta_{ij} - \frac{t_i}{R_i(t_1, \dots, t_k)} \frac{\partial R_i}{\partial t_j}(t_1, \dots, t_k)\,.$$

Before moving on, we need to define the convolutional power

$$g(\mathbf{k})^{*n} = g(\mathbf{k})^{*n-1} * g(\mathbf{k}) \qquad g(\mathbf{k})^{*0} = \delta(\mathbf{k})\,,$$

where we define the convolution as

$$c(\mathbf{k}) = (f * g)(\mathbf{k}) \qquad c(\mathbf{k}) = \sum_{\mathbf{r}+\mathbf{m}=\mathbf{k}} f(\mathbf{r}) g(\mathbf{m}) = [\mathbf{x}^\mathbf{k}] F(\mathbf{x}) G(\mathbf{x})\,.$$

We can now state the main theorem of the section. We will state the following theorem only for black nodes, with a reminder that every other system is completely symmetric and solves in exactly the same way. Indeed the final solution obtained from a system is the same for all other systems, one just needs to swap the correct elements.

Theorem 4.5.3. *Let $W_B(x,y)$ be the generating function as defined in Section 4.2. Then*

$$\begin{aligned}[x^b y^r]W_B(x,y) &= w_B(b,r)\\ &= u_b(k,l) * u_b'(k,l)^{*(i-1)} * u_r'(k,l)^{*(j-1)} * d(k,l)\mid_{k=b-1,l=r},\end{aligned}$$

where

$$d(k,l) = \left[u_b'(k,l) - ku_b'(k,l)\right] * \left[u_r'(k,l) - lu_r'(k,l)\right] - lu_b'(k,l) * ku_r'(k,l),$$

with u_b' and u_r' generated by $\partial_x U_B$ and $\partial_x U_R$ respectively.

Proof. Since we don't need to differentiate between different excess distributions, we will lighten the notation by redefining

$$\partial_x U_B(x,y) = U_B'(x,y) \quad \text{and} \quad \partial_x U_R(x,y) = U_R'(x,y)$$

$$\partial_x W_B(x,y) = W_B'(x,y) \quad \text{and} \quad \partial_x W_R(x,y) = W_R'(x,y).$$

Then, following Good's formalism we define

$$R(x,y) = [R_1(x,y), R_2(x,y)] = \left[U_B'(x,y), U_R'(x,y)\right],$$

$$A(x,y) = [A_1(x,y), A_2(x,y)] = \left[W_B'(x,y), W_R'(x,y)\right].$$

One can easily see that these formal series, given the system (4.11), satisfy the condition (4.15). Lastly, if we define

$$F_B(x,y) = U_B(x,y).$$

By applying Theorem (4.5.2) we obtain

$$\begin{aligned}[x^b y^r]\frac{W_B}{x} &= [x^b y^r]U_B(W_B', W_R') && \text{by 4.11}\\ &= [x^b y^r]F_B[A(x,y)]\\ &= [t^b s^r]F_B(t,s)\det K(t,s)(R_1(t,s))^b(R_2(t,s))^r && \text{by the G-LIF}\\ &= [t^b s^r]U_B(t,s)\left[\det K(t,s)U_B'U_R'\right](U_B')^{b-1}(U_R')^{r-1}.\end{aligned}$$

Moreover we will have that

$$K(t,s) = \begin{bmatrix} 1 - \frac{t}{U_B'}\frac{\partial U_B'}{\partial t} & -\frac{t}{U_B'}\frac{\partial U_B'}{\partial s} \\ -\frac{s}{U_R'}\frac{\partial U_R'}{\partial t} & 1 - \frac{s}{U_R'}\frac{\partial U_R'}{\partial s}, \end{bmatrix} \tag{4.16}$$

and therefore

$$\left[\det KU_B'U_R'\right] = (U_B' - t\frac{\partial U_B'}{\partial t})(U_R' - s\frac{\partial U_R'}{\partial s}) - s\frac{\partial U_B'}{\partial s}\,t\frac{\partial U_R'}{\partial t},$$

given that

$$
\begin{aligned}
t\frac{\partial U'_B}{\partial t}(t,s) &= \sum_{k,l\in\mathbb{N}_0} u'_b(k,l)t\frac{\partial}{\partial t}(t^k s^l) = \sum_{k,l\in\mathbb{N}_0} u'_b(k,l)kt^k s^l\,,\\
s\frac{\partial U'_R}{\partial s}(t,s) &= \sum_{k,l\in\mathbb{N}_0} u'_r(k,l)s\frac{\partial}{\partial s}(t^k s^l) = \sum_{k,l\in\mathbb{N}_0} u'_r(k,l)lt^k s^l\,,\\
s\frac{\partial U'_B}{\partial s}(t,s) &= \sum_{k,l\in\mathbb{N}_0} u'_b(k,l)s\frac{\partial}{\partial s}(t^k s^l) = \sum_{k,l\in\mathbb{N}_0} u'_b(k,l)lt^k s^l\,,\\
t\frac{\partial U'_R}{\partial t}(t,s) &= \sum_{k,l\in\mathbb{N}_0} u'_r(k,l)t\frac{\partial}{\partial t}(t^k s^l) = \sum_{k,l\in\mathbb{N}_0} u'_r(k,l)kt^k s^l\,.
\end{aligned}
$$

We then have that $[\det K(t,s)U'_B(t,s)U'_R(t,s)]$ generates the sequence

$$
d(k,l) = \left[u'_b(k,l) - ku'_b(k,l)\right] * \left[u'_r(k,l) - lu'_r(k,l)\right] - lu'_b(k,l) * ku'_r(k,l)\,, \tag{4.17}
$$

therefore

$$
\begin{aligned}
w_B(b+1,r) &= [x^b y^r]\frac{W_B(x,y)}{x} && (4.18)\\
&= u_b(k,l) * u'_b(k,l)^{*(i-1)} * u'_r(k,l)^{*(j-1)} * d(k,l)\mid_{k=b,l=r}\,. && (4.19)
\end{aligned}
$$

□

As a corollary we can state

Corollary 4.5.4. *Let $w_B(n)$ be the size distribution of weakly connected components for a bigraph with degree distributions generated by Equation* (4.4)*. Then*

$$
w_B(n) = \sum_{b+r=n-1} w_B(b,r)\,,
$$

where $w_B(b,r)$ is generated by $W_B(x,y)$ as defined in Section 4.2.

For the proof we refer to Section 4.2.1.

Chapter 5

Numerical Analysis and Algorithm

Following the main idea, generating random graphs and reading out the connected components provides an approximate numerical solution to Smoluchowski's infinite system of equations. Numerically solving the system of ODEs directly falls victim to the curse of dimensionality, especially for systems with many different components, and it requires a cutoff. Since the original theoretical system is composed of an infinite number of equations, this also leads to inaccurate solutions, given the mean-field nature of the system where every component interacts with the others.

5.1 The Algorithm

Let us introduce the *Chung-Lu* random graph model. It is a generalised Erdös-Renyi random graph in which every node u is assigned a weight w_u. We define the mean weight $\bar{w} = \sum_u w_u/N$, and two nodes u and v with weights w_u and w_v are joined together with probability $p_{u,v} = w_u w_v/\bar{w}N$. The expected degree of the node u is then $\sum_{v\neq u} w_u w_v/\bar{w}N = w_u - w_u^2/\bar{w}N$, which for very large graphs converges to w_u. Therefore the weight w_u represents the expected degree of the node u in an infinite graph. Also in a Chung-Lu model, the expected amount of edges is then $M = N\bar{w}/2$. From this we can quickly see that Erdös-Renyi random graphs are particular Chung-Lu random graphs with $p_{u,v} = p = c/N$.

In our model, we define a matrix A that has as entries the rates a_{ij} which describe how likely two nodes of type i and j are to form a link. The same rates also appear (properly renamed) in the degree distributions (4.4) used in our model

$$U_B(x,y) = e^{a_{11}t(x-1)}e^{a_{12}t(y-1)}\,,$$

$$U_R(x,y) = e^{a_{21}t(x-1)}e^{a_{22}t(y-1)}\,.$$

But in particular, the quantities ta_{ij} define the expected ij-degrees (that is, the expected number of edges from nodes of type i to nodes of type j.) Taking a step back, if we have a multicoloured graph, we can reconstruct it by bundling different types

of edges together. That is, first we remove all edges, and then, for every pair i, j we go through the nodes of type i and place back all edges that go from nodes of type i to nodes of type j. We can then leverage the Chung-Lu model and see each iteration as constructing a graph between two sets of nodes with weights $c_{ij} := ta_{ij}$ and $c_{ji} := ta_{ji}$ respectively.

Let G be a multicoloured graph, with N total nodes. Since we have more than one colour we will have a set of positive integers $\{n_1, \ldots, n_d\}$ such that $\sum_i n_i = N$ that describes the frequency of i-coloured nodes in the graphs. Without loss of generality we can relabel nodes of type i with numbers from $\sum_{k<i} n_k$ to $\sum_{k\leq i} n_k$. Therefore we partition the set $[N] = \{1, 2, \ldots, N\}$ into d subsets of length n_i respectively.

$$[N] = (\quad [n_1] \quad | \quad [n_2] \quad | \quad \ldots \quad | \quad [n_d] \quad).$$

We can then adapt an algorithm from [MH11] and define a procedure that connects two types of nodes, presented below:

Algorithm 1 Chung-Lu Graph

Ensure: $0 \leq c_1 \leq n_2 - 1, \quad 0 \leq c_2 \leq n_1 - 1$ ▷ no more edges than nodes
  procedure CHUNG-LU-EDGES(c_{ij}, c_{ji}, n_i, n_j)
    $E_{ij} \leftarrow \emptyset$
    $S_i \leftarrow c_{ij} n_i$
    $S_j \leftarrow c_{ji} n_j$
    for $u = 1$ to $n_i - 1$ **do**
      $v \leftarrow u + 1$
      $p \leftarrow \min(c_{ij} c_{ji} / S_i, 1)$
      while $v \leq n_j$ and $p > 0$ **do**
        if $p \neq 1$ **then**
          choose $r \in (0, 1)$ uniformly at random
          $v \leftarrow v + \left\lfloor \frac{log(r)}{log(1-p)} \right\rfloor$
        end if
        if $v \leq n_j$ **then**
          $q \leftarrow \min(c_{ij} c_{ji} / S_j, 1)$
          choose $r \in (0, 1)$ uniformly at random
          if $r < q/p$ **then**
            $E_{ij} \leftarrow E_{ij} \cup (u, v)$ ▷ edges are ordered pairs
          end if
          $p \leftarrow q$
          $v \leftarrow v + 1$
        end if
      end while
    end for
  return E_{ij} ▷ The edges will have relative numbering
  end procedure

This procedure returns a set of pseudo-edges that stem from the n_i nodes of type i and arrive in one of the n_j nodes of type j. The order of the elements in a pseudo-edge is important since we will need to place them back into the graph in the proper manner, for the moment a pseudo-edge $(u, v) \in E_{ij}$ represents the edge from the u-th node of type i to the v-th node of type j. The algorithm to generate a multicoloured graph with d colours will then consists in generating d^2 sets of pseudo-edges E_{ij}, one for each pair (i, j), from nodes of type i to nodes of type j and then correctly map them back to the main graph.

Algorithm 2 d-coloured graph with N nodes

$E_{ij} \leftarrow \emptyset$ for every pair (i, j)
for all (i, j) pairs, $i, j \leq d$ **do**
  $E_{i,j} \leftarrow$ CHUNG-LU-EDGES$(c_{ij}, c_{ji}, n_i, n_j)$
end for
for all E_{ij} **do**
  for all $(u, v) \in E_{ij}$ **do**
    $E \leftarrow E \cup \{\sum_{k<i} n_k + u, \sum_{k<j} n_k + v\}$
  end for
end for

Theorem 5.1.1. *Let N be the total number of nodes, d the number of colours. When run for weights $c_{ij} = ta_{ij}$ before the gelation time $t \leq t_c$, the Algorithm 2 runs in $O((d+1)N)$ expected time*

Proof. The average number of nodes of a certain colour is $\bar{n} = N/d$. We know that the maximum amount of edges in the finished graph is $M = O(N/2)$ since it is when we encounter the giant component, each pair (i, j) will be on average responsible for adding $\bar{m} := O(M/d^2)$ edges to the final graph. The procedure CHUNG-LU-EDGES runs through the first loop on average $\bar{n} - 1$ times, and the inner loop only runs for $\bar{m}$ iterations on average [MH11]. We run the procedure d^2 times, one for each pair (i, j). Lastly, we cycle through all the pseudo-edges to map them to the corresponding edge. Therefore adding all together

$$d^2(\bar{n} + \bar{m}) + M \leq d^2\left(\frac{N}{d} + \frac{N}{2d^2}\right) + \frac{N}{2} = dN + N\,.$$

□

Remark. Each of the d^2 runs is independent from the others. That means that we can easily generate the d^2 pseudo-edgeset concurrently, furthering reducing the time needed.

5.2 Numerical Results

We implemented the algorithm discussed above using the Julia language version 1.7.0. The code used in this section can be found in the GitHub repository `https://github.com/ghyatzo/random-graph-smoluchowski-thesis`.

The matrix A in the kernel allows us to specify very different behaviours of our graphs. For example, we could wish for a uniform chance of linkage between all types of nodes, or only allow specific connections to be made, of which we can also decide the intensity. These are some of the examples

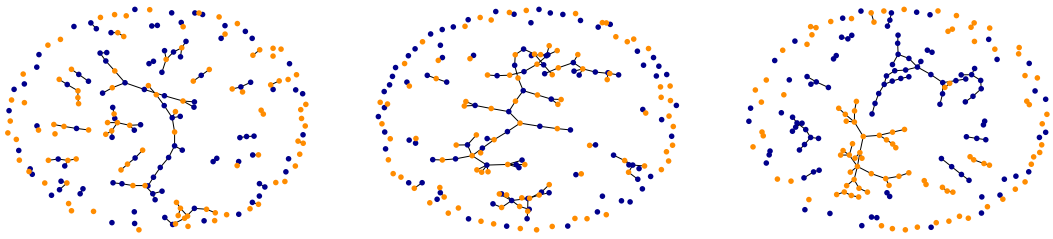

(a) Homogeneous (b) Alternating (c) Separate

which corresponds to the matrices at time $t = 1$

$$\begin{bmatrix} 0.5 & 0.5 \\ 0.5 & 0.5 \end{bmatrix} \qquad \begin{bmatrix} 0 & 1 \\ 1 & 0 \end{bmatrix} \qquad \begin{bmatrix} 1 & 0 \\ 0 & 1 \end{bmatrix}$$

And indeed we see giant components, each one with characteristics described by the respective matrix. And the possibilities only grow with more components.

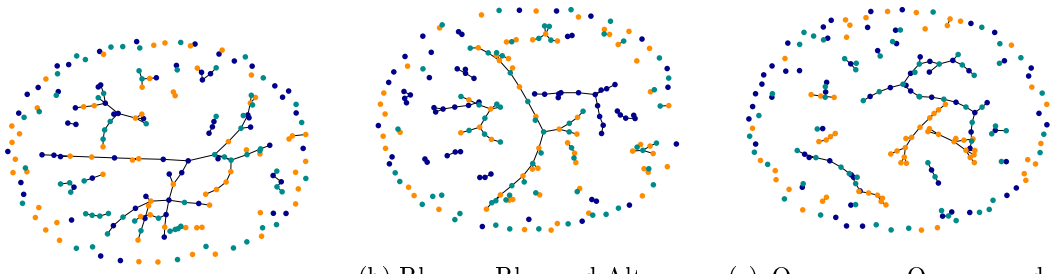

(a) Homogeneous (b) Blue on Blue and Alternating Orange-Cyan (c) Orange on Orange and Alternating Blue-Cyan

which corresponds to the matrices at time $t = 1$

$$\begin{bmatrix} \frac{1}{3} & \frac{1}{3} & \frac{1}{3} \\ \frac{1}{3} & \frac{1}{3} & \frac{1}{3} \\ \frac{1}{3} & \frac{1}{3} & \frac{1}{3} \end{bmatrix} \qquad \begin{bmatrix} 1 & 0 & 0 \\ 0 & 0 & 1 \\ 0 & 1 & 0 \end{bmatrix} \qquad \begin{bmatrix} 0 & 0 & 1 \\ 0 & 1 & 0 \\ 1 & 0 & 0 \end{bmatrix}$$

5.2.1 Methodology and parameters

All the various possible configurations are plentiful, and visualising a specific configuration and its evolution in its entirety for every parameter variation would require a harrowing amount of plots or more dimensions than our brain can comprehend. We will therefore need some default parameters to work with. The simulations were performed with $N = 10^6$ nodes with $N/2$ black nodes and $N/2$ red nodes. The kernel used is

$$A_{(2)} = \begin{bmatrix} 1 & 0.9 \\ 0.9 & 1 \end{bmatrix},$$

which according to Theorem 3.1.2 will generate a giant component at $t_c = \frac{1}{||A||} \approx 0.526$. To smooth out the inherent variability of the algorithm, we will generate 50 graphs with the same parameters, read out the necessary information and average them.

To generate a baseline close to the ground truth to test our algorithm, we numerically integrate Smoluchowski's system of ODEs with a cutoff at component size of 100, using the Tsitouras 5/4 Runge-Kutta method. The system was solved with normalized monodispersed initial conditions $w_{e_i}(0) = 1$.

An arbitrarily chosen fixed time of $t = 0.39$ was chosen to run simulations shown in Figures 5.3 to 5.7. In the time complexity analysis section, we also generate 3-coloured graphs for comparison, we use $N = 10^6$ with an even partitioning $n_1 = n_2 = n_3 = \frac{1}{3}N$. The kernel used is

$$A_{(3)} = \begin{bmatrix} 1 & 0.9 & 0.9 \\ 0.9 & 1 & 0.9 \\ 0.9 & 0.9 & 1 \end{bmatrix}.$$

Which has a critical time of $t_c \approx 0.357$. Since the time complexity depends on the amount of edges created, and the amount of edges depends on the critical time, we normalise the kernel $A_{(3)}$ such that it has the same critical time as $A_{(2)}$, therefore

$$\tilde{A}_{(3)} = A_{(3)} \frac{||A_{(2)}||}{||A_{(3)}||}.$$

5.2.2 Weakly-connected component study

At the start, the number of connected components is very low, and all the mass is concentrated in w_1. As we let the system evolve, we see a shift towards the tail of the distribution, and finally, at the critical time, the plot shows a significantly different shape than the previous two. We indeed reach a heavy tail phase, encountering a *run away growth*, or the so-called *gelation*.

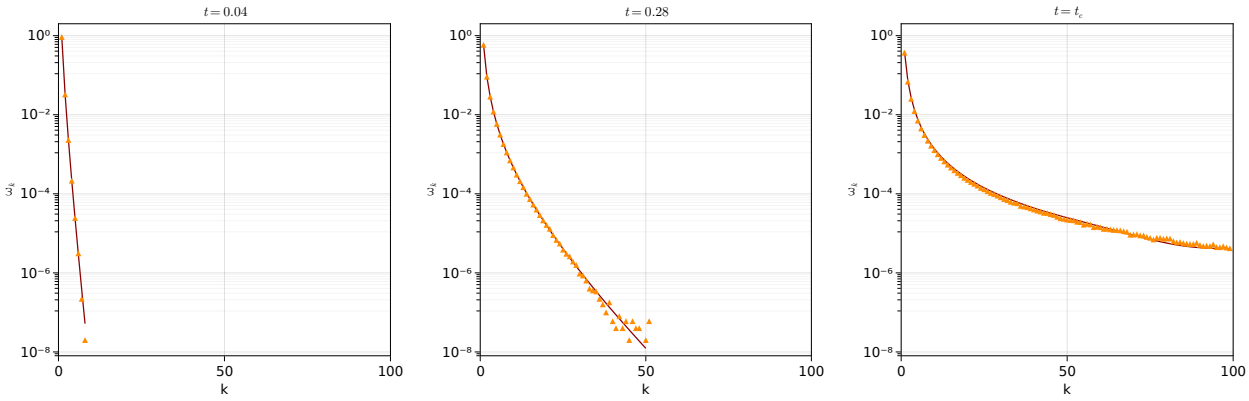

Figure 5.3: The weak components density at 3 different points in time during the evolution of the system. where we compare the connected components of a bigraph (orange triangles) and the solution to the ODE system (red solid line).

One might notice, especially in the middle figure, that in the tail, the distribution shows high variability. This is due to a lack of resolution of the bigraph. Indeed, we are approximating an infinite graph with a finite amount of nodes, therefore the maximum component size we can obtain is directly dependent on the total amount of nodes. If we refine the subcritical window with $p = (1 - \varepsilon)/N$ and $\varepsilon = \lambda N^{-1/3}$ for $\lambda \to N^{1/3}$ the expected maximum component size follows $O(N^{2/3}\lambda^{-2}\ln(\lambda))$.

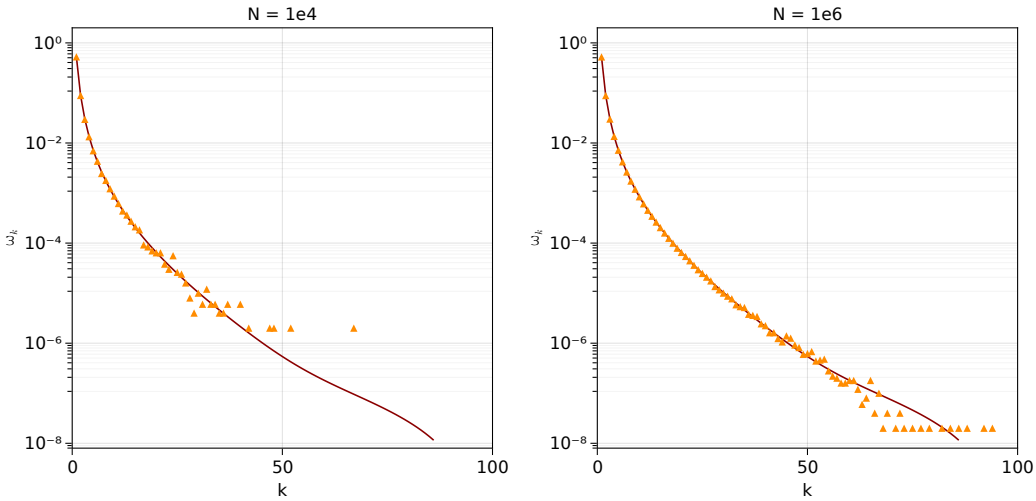

Figure 5.4: The weak components density for 3 differently sized bigraphs at a fixed time $t = 39$. (orange triangles) connected components, (solid line) ODE solution

5.2.3 Error convergence and time complexity

Increasing the total number of nodes, not only helps with the maximum components we can see but also increases the accuracy of our approximations.

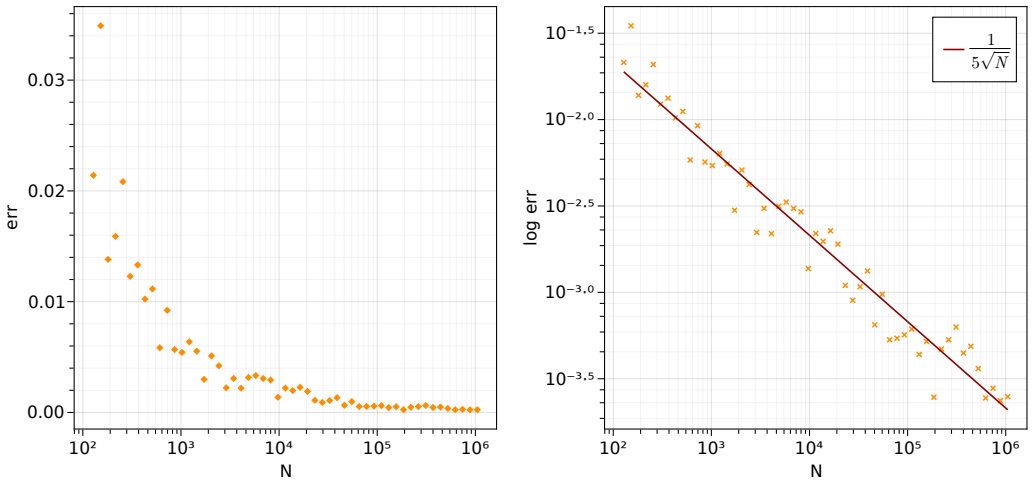

Figure 5.5: The convergence towards 0 of the absolute cumulative error for increasing values of N

The cumulative absolute error is the sum of the absolute differences between the connected components distribution and the ODE solution across all densities. We can see a quick drop in the error at the initial steps but, as expected, adding more nodes is less effective each subsequent time. The log-log plot suggests an $O(N^{\alpha})$ error scaling. Fitting a power law model $y = \beta x^{\alpha}$ through simple log-linear regression we obtain

$$\alpha \approx -0.502 \qquad \beta \approx 0.214$$

which supports an $O(N^{-1/2})$ error scaling. In the plot, we add a red line representing the function $y = \frac{1}{5\sqrt{N}}$ as a visual comparison.

Of course, increasing the total number of nodes comes with the tradeoff of increased computation time. We know from Theorem 5.1.1 that time grows linearly with the number of nodes for a given dimension d. In the classic time vs. memory tradeoff, to generate very big graphs available memory is the limiting factor. Indeed, in Figure 5.6a we plot the runtime needed (in seconds) to generate each graph, together with the time spent by the machine managing its own memory. These simulations were run on a machine with only 16Gb of RAM, which showed to be insufficient for $N \geq 10^6$. A more solid approach, shown in Figure 5.6b, consists on counting the number of iterations needed by the Algorithm 2 to generate a graph.

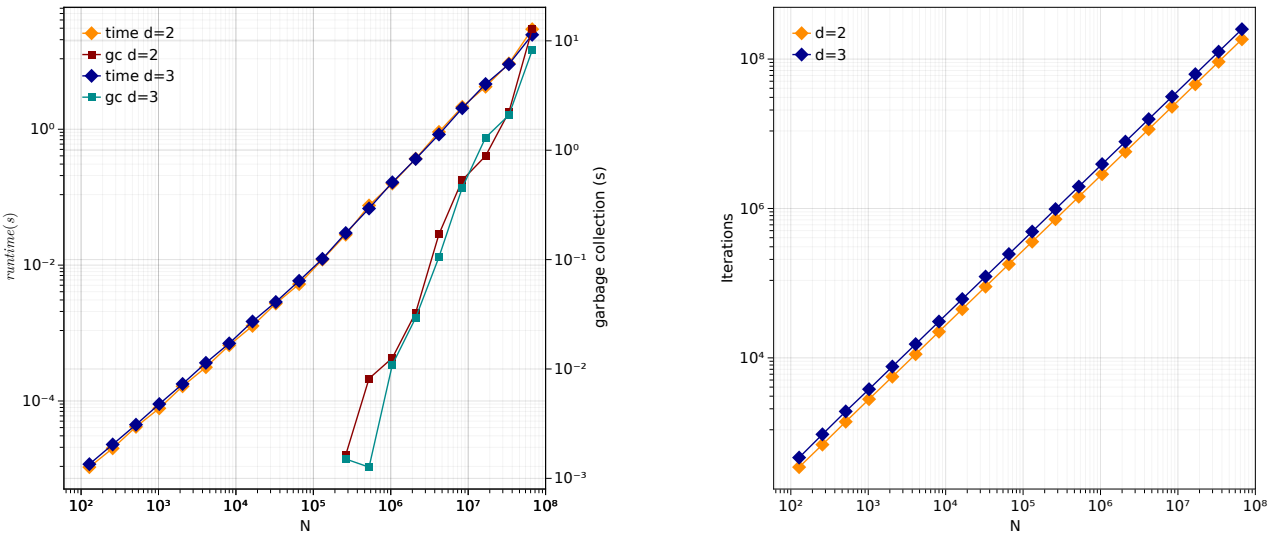

(a) Time

(b) Iterations

Figure 5.6: Linear time evolution for increasing N, and the memory bottleneck represented by the activity of the machine's garbage collection routines.

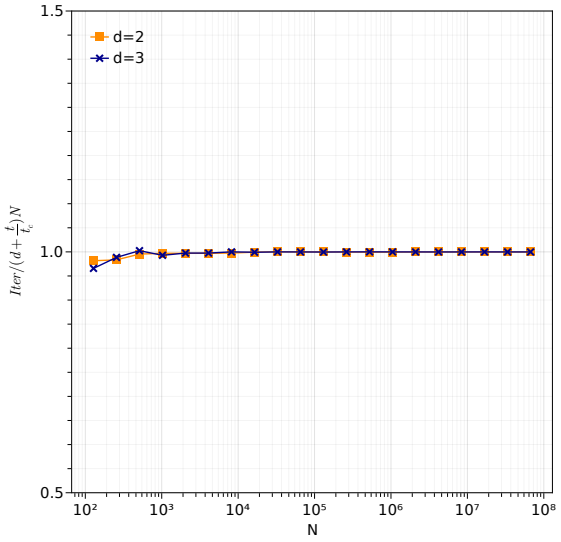

Figure 5.7: The Coefficient for the algorithmic complexity for $t = 0.39$ and $t_c = 0.526$

Knowing we have an algorithmic complexity of $O((d+1)N)$ it is interesting to check what is the coefficient. We do this by plotting the iterations for each N against $(d+1)N$. In this specific case, since we normalised to the same critical time (see section 5.2.1), we refine the algorithmic complexity estimate to $O\left((d+\frac{t}{t_c})N\right)$.

5.2.4 Components composition and Burgers' equation

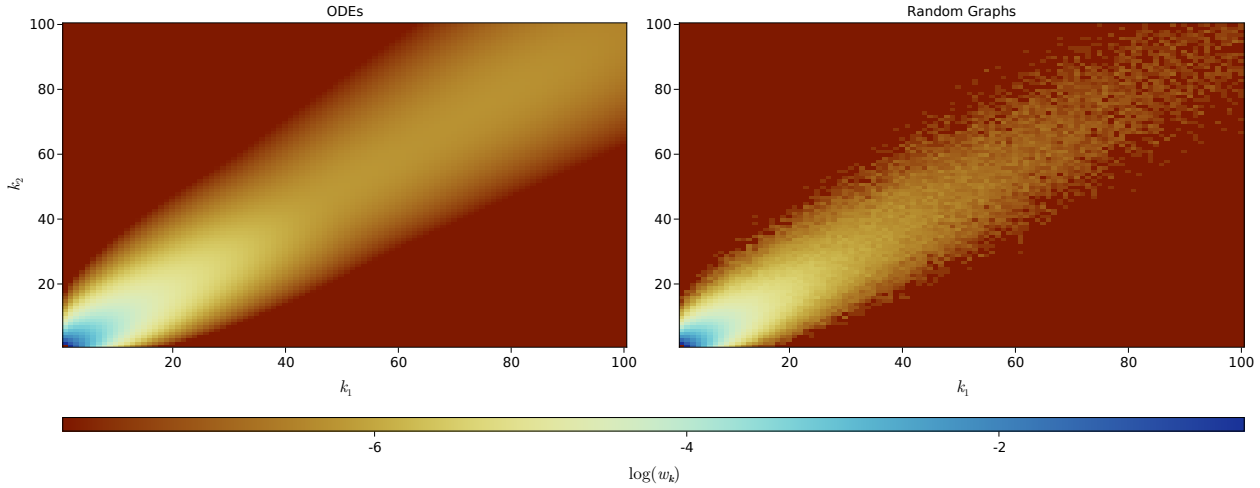

Figure 5.8: Log distribution $w_{\mathbf{k}}$ of the specific compositions of objects $\mathbf{k} = (k_1, k_2)$ at $t = 0.52$ with kernel $A_{(2)}$

Although much rougher, due to the discrete approximation, the random graph data correctly approximates the data obtained through more classical approaches. Both dimensional distributions of the components show a clear propagation along the diagonal. A natural question is asking what parameters affect the shape of the distribution. Unfortunately, we still can't answer this question in detail but we can argue through some experiments that both the kernel and the node distribution play a role.

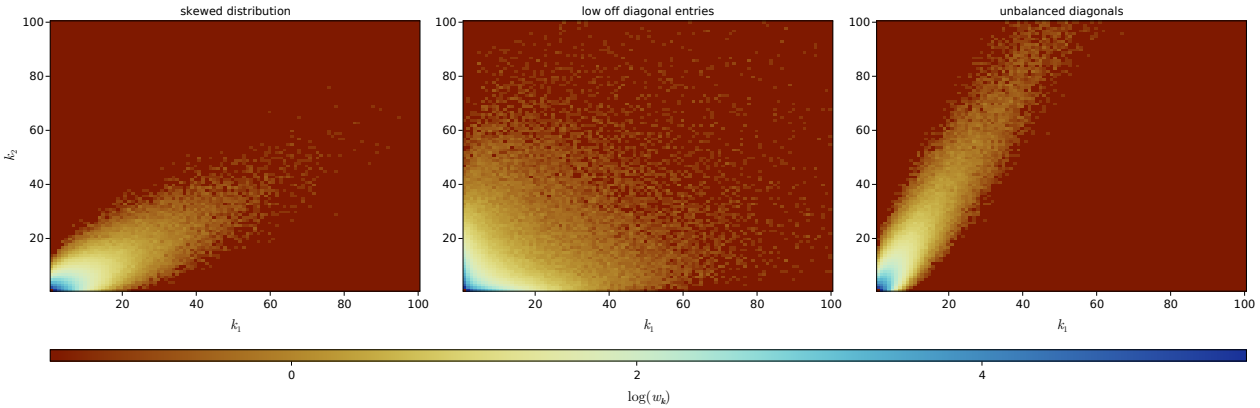

Figure 5.9: Log distribution $w_{\mathbf{k}}$ of the specific compositions of objects $\mathbf{k} = (k_1, k_2)$ for some different kernels and distributions at $t = 0.52$

In Figure 5.9 we tested three different scenarios: in the leftmost picture, we used the usual $A_{(2)}$ kernel but with a skewed distribution of nodes such that we had 70% of type 1 nodes and 30% of type 2 nodes. In the middle picture, a balanced population with a kernel with very low off-diagonal entries was used,

$$\begin{bmatrix} 1.0 & 0.1 \\ 0.1 & 1.0 \end{bmatrix}.$$

Lastly in the rightmost picture we used a balanced node population and a kernel with very skewed diagonal entries

$$\begin{bmatrix} 0.2 & 0.5 \\ 0.5 & 1.0 \end{bmatrix}.$$

All kernels were normalised to retain the critical time at $t_c = 0.526$ as $A_{(2)}$. We clearly see some effects, on the angle of growth, when we tweak either the population balance or the diagonal entry symmetry, and on the spread of the distribution, when we tweak the off-diagonal entries magnitude.

Burgers' equation for weakly-connected components

From Section 2.1.1 we map Smoluchowski's problem into a Burgers' inviscid equation. Following this idea into the simulations, we can compose the weak components data obtained either from the system of ODEs or the random graphs approaches into the solution of the initial value problem

$$\begin{cases} u_t + (u-1)u_z = 0 \\ u(0) = e^{-z} \qquad\qquad z \geq 0 \end{cases}.$$

In Figure 5.10 we can see that both approaches correctly predict the discontinuity or shock in the solution, represented by the blow up of the derivative at 0 the closer we get to the critical time t_c.

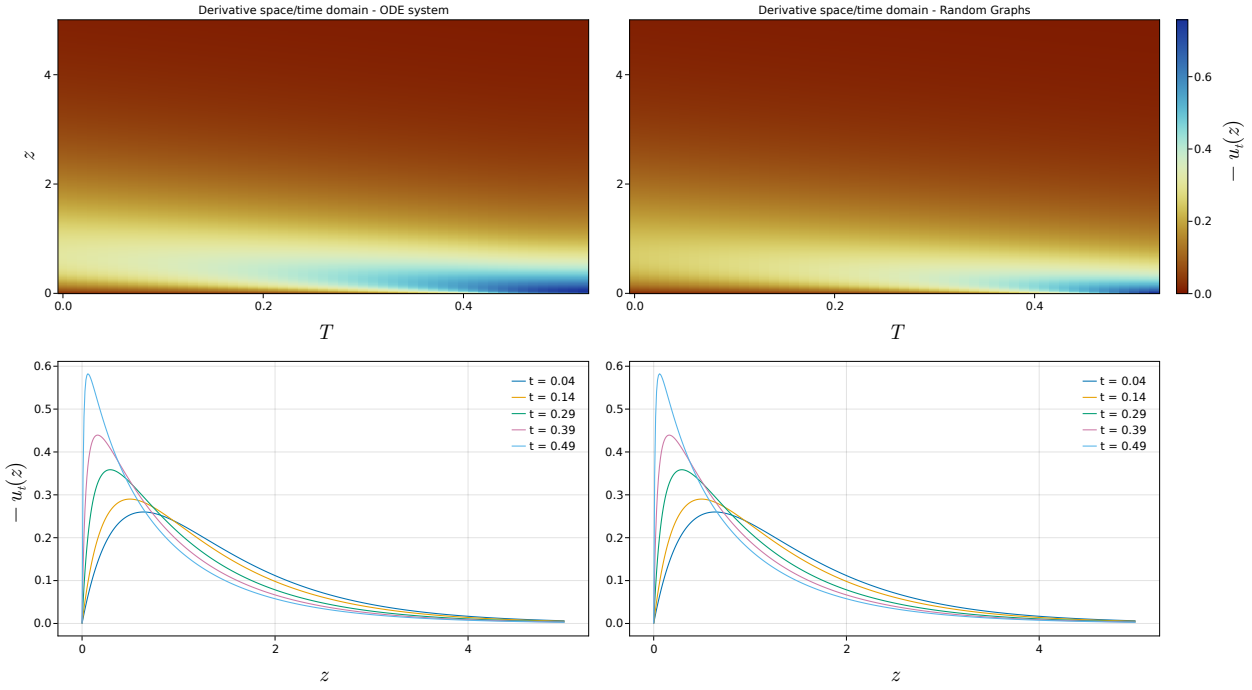

Figure 5.10: Space/Time Domain and cross-sections of $u_t = -u_z(u-1)$ with $u(z,0) = e^{-z}$

Further Research

In many parts of this manuscript, we had to restrict the focus to specific conditions to ease the treatment. Even with this very narrow focus, there are still many questions to answer or parts to expand.

Probably one of the most important questions that will need further work is figuring out what happens when we start from different initial conditions that are not monodisperse. It is unclear how different initial degree configurations would affect the evolution of the distribution as a whole, and consequently the rest of the system. But, perhaps more importantly, it could allow us to extend such results to different initial conditions for the inviscid Burgers' equation.

More research will also be needed towards extending the model and introducing extra terms, for example, a diffusion term, and the analysis that follows.

Central to the whole derivation is the quantity e^{-x} that seems to play a central role. Indeed, the generating functions that we use in the first part of the manuscript include this transformation $G(e^{-x})$. Better understanding the overarching implications of this transformation in this setting could bring useful insights.

Properly analyse the close form solution obtained in Chapter 4 could give exact solutions to the multicomponent multiplicative coalescence problem, which is useful to test the accuracy of various numerical schemes.

One other venue of further exploration is asking how well we could approximate other more complicated kernels through a linear decomposition of bilinear forms, and see if that translates well with the Smoluchowski's system.

Lastly, from the brief numerical experiments, we noticed that we can manipulate the shape of the distribution through the parameters of the system. A promising venue, that was not explored due to time constraints, could be some form of correlation parameter to describe the angle and spread of the "beam" of the distribution.

In short, too much to do, too little time.

Bibliography

[ADB09] Menwer Attarakih, Christian Drumm, and Hans-Jörg Bart. Solution of the population balance equation using the sectional quadrature method of moments (sqmom). *Chemical Engineering Science*, 64:742–752, 2009.

[Ahr20] Robin Ahrens. *Efficient numerical treatment of aggregation integrals in multivariate population balance equations.* PhD thesis, Technischen Universität Hamburg, 2020.

[Ald99] David J. Aldous. Deterministic and stochastic models for coalescence (aggregation and coagulation): a review of the mean-field theory for probabilists. *Bernoulli*, 5(1):3 – 48, 1999.

[AS00] Noga Alon and Joel Spencer. *The probabilistic method.* Wiley-Interscience Series in Discrete Mathematics. John Wiley & Sons, Nashville, TN, 2 edition, September 2000.

[Bab99] Hans Babovsky. On a monte carlo scheme for smoluchowski's coagulation equation. *Monte Carlo Methods Appl.*, 5(1):1–18, 1999.

[Ber02] Jean Bertoin. Eternal solutions to smoluchowski's coagulation equation with additive kernel and their probabilistic interpretations. *Ann. Appl. Probab.*, 12(2):547–564, May 2002.

[BH98] Craig F Bohren and Donald R Huffman. *Absorption and scattering of light by small particles.* John Wiley & Sons, Nashville, TN, April 1998.

[BKB+15] Nikolai Brilliantov, P L Krapivsky, Anna Bodrova, Frank Spahn, Hisao Hayakawa, Vladimir Stadnichuk, and Jürgen Schmidt. Size distribution of particles in saturn's rings from aggregation and fragmentation. *Proc. Natl. Acad. Sci. U. S. A.*, 112(31):9536–9541, August 2015.

[BLL97] F. Bergeron, Gilbert Labelle, and Pierre Leroux. Combinatorial species and tree-like structures. In *Encyclopedia of mathematics and its applications*, 1997.

[BR15] Béla Bollobás and Oliver Riordan. An old approach to the giant component problem. *J. Combin. Theory Ser. B*, 113:236–260, July 2015.

[CF11] Eduardo Cepeda and Nicolas Fournier. Smoluchowski's equation: Rate of convergence of the Marcus–Lushnikov process. *Stoch. Process. Their Appl.*, 121(6):1411–1444, June 2011.

[DFT02] Madalina Deaconu, Nicolas Fournier, and Etienne Tanré. A pure jump markov process associated with smoluchowski's coagulation equation. *Ann. Probab.*, 30(4):1763–1796, October 2002.

[Dra72] Ronald L Drake. A general mathematical survey of the coagulation equation. In G.M. HIDY and J.R. BROCK, editors, *Topics in Current Aerosol Research*, International Reviews in Aerosol Physics and Chemistry, pages 201–376. Pergamon, 1972.

[ER59] P Erdös and A Rényi. On random graphs i. *Publicationes Mathematicae Debrecen*, 6:290–297, 1959.

[EW01] Andreas Eibeck and Wolfgang Wagner. Stochastic particle approximations for smoluchoski's coagualtion equation. *Ann. Appl. Probab.*, 11(4):1137–1165, November 2001.

[FDGG07] J M Fernández-Díaz and G J Gómez-García. Exact solution of smoluchowski's continuous multi-component equation with an additive kernel. *EPL*, 78(5):56002, June 2007.

[FDGG10] Julio M Fernández-Díaz and Germán J Gómez-García. Exact solution of a coagulation equation with a product kernel in the multicomponent case. *Physica D*, 239(5):279–290, March 2010.

[FG04a] Nicolas Fournier and Jean-Sébastien Giet. Convergence of the Marcus-Lushnikov Process. *Methodology and Computing in Applied Probability*, pages 219–231, 2004.

[FG04b] Nicolas Fournier and Jean-Sébastien Giet. Exact simulation of nonlinear coagulation processes. *Monte Carlo Methods Appl.*, 10(2), January 2004.

[Fil61] A F Filippov. On the distribution of the sizes of particles which undergo splitting. *Theory Probab. Appl.*, 6(3):275–294, January 1961.

[FLNV21a] Marina A Ferreira, Jani Lukkarinen, Alessia Nota, and Juan J L Velázquez. Localization in stationary non-equilibrium solutions for multicomponent coagulation systems. *Commun. Math. Phys.*, 388(1):479–506, November 2021.

[FLNV21b] Marina A Ferreira, Jani Lukkarinen, Alessia Nota, and Juan J L Velázquez. Multicomponent coagulation systems: existence and nonexistence of stationary non-equilibrium solutions. March 2021.

[FM77] S K Friedlander and William H Marlow. Smoke, dust and haze: Fundamentals of aerosol behavior. *Phys. Today*, 30(9):58–59, September 1977.

[GL96] David Ginter and Sudarshan K. Loyalka. Apparent size-dependent growth in aggregating crystallizers. *Chemical Engineering Science*, 51:3685–3695, 1996.

[Gor88] Deborah M Gordon. Group-level exploration tactics in fire ants. *Behaviour*, 104(1-2):162–175, 1988.

[HRM88] M J Hounslow, R L Ryall, and V R Marshall. A discretized population balance for nucleation, growth, and aggregation. *AIChE J.*, 34(11):1821–1832, November 1988.

[ILHE01] Simon M Iveson, James D Litster, Karen Hapgood, and Bryan J Ennis. Nucleation, growth and breakage phenomena in agitated wet granulation processes: a review. *Powder Technol.*, 117(1-2):3–39, June 2001.

[KKPS93] F Einar Kruis, Karl A Kusters, Sotiris E Pratsinis, and Brian Scarlett. A simple model for the evolution of the characteristics of aggregate particles undergoing coagulation and sintering. *Aerosol Sci. Technol.*, 19(4):514–526, January 1993.

[Kry17] Ivan Kryven. General expression for the component size distribution in infinite configuration networks. *Phys. Rev. E.*, 95(5-1):052303, May 2017.

[LCT49] Paco A. Lagerstrom, Julian D. Cole, and Leon Trilling. Problems in the theory of viscous compressible fluids. 1949.

[LDG98] Shouci Lu, Yuqing Ding, and Jinyong Guo. Kinetics of fine particle aggregation in turbulence. *Adv. Colloid Interface Sci.*, 78(3):197–235, November 1998.

[Lee00] M Lee. On the validity of the coagulation equation and the nature of runaway growth. *Icarus*, 143(1):74–86, January 2000.

[Lis93] Jack J Lissauer. Planet formation. *Annu. Rev. Astron. Astrophys.*, 31(1):129–172, September 1993.

[Lus73] A A Lushnikov. Evolution of coagulating systems. *J. Colloid Interface Sci.*, 45(3):549–556, December 1973.

[Lus78] A A Lushnikov. Coagulation in finite systems. *J. Colloid Interface Sci.*, 65(2):276–285, June 1978.

[Mar68] Allan H Marcus. Stochastic coalescence. *Technometrics*, 10(1):133, February 1968.

[MB92] J Mydlarz and D Briedis. Growth rate dispersion vs size-dependent growth rate for MSMPR crystallizer data. *Comput. Chem. Eng.*, 16(9):917–922, September 1992.

[MH11] Joel C Miller and Aric Hagberg. Efficient generation of networks with given expected degrees. In *Lecture Notes in Computer Science*, Lecture notes in computer science, pages 115–126. Springer Berlin Heidelberg, Berlin, Heidelberg, 2011.

[MLK06] Themis Matsoukas, Kangtaek Lee, and Taehoon Kim. Mixing of components in two-component aggregation. *AIChE J.*, 52(9):3088–3099, September 2006.

[Mül28] Hans Müller. Zur allgemeinen theorie ser raschen koagulation. *Fortschrittsberichte über Kolloide Polym.*, 27(6-12):223–250, November 1928.

[MZTS16] Sergey A Matveev, Dmitry A Zheltkov, Eugene E Tyrtyshnikov, and Alexander P Smirnov. Tensor train versus monte carlo for the multicomponent smoluchowski coagulation equation. *J. Comput. Phys.*, 316:164–179, July 2016.

[Niw98] H S Niwa. School size statistics of fish. *J. Theor. Biol.*, 195(3):351–361, December 1998.

[Nor99] James R Norris. Smoluchowski's coagulation equation: uniqueness, nonuniqueness and a hydrodynamic limit for the stochastic coalescent. *Ann. Appl. Probab.*, 9(1):78–109, February 1999.

[OKMO+13] T Olenius, O Kupiainen-Määttä, I K Ortega, T Kurtén, and H Vehkamäki. Free energy barrier in the growth of sulfuric acid-ammonia and sulfuric acid-dimethylamine clusters. *J. Chem. Phys.*, 139(8):084312, August 2013.

[OS78] Norman Owen-Smith. The african buffalo. a study of resource limitation of populations. a. r. e. sinclair. *Q. Rev. Biol.*, 53(2):187–187, June 1978.

[PK10] H R Pruppacher and J D Klett. Cloud electricity. In *Microphysics of Clouds and Precipitation*, pages 792–852. Springer Netherlands, Dordrecht, 2010.

[QS90] Gerald D Quinlan and Stuart L Shapiro. The dynamical evolution of dense star clusters in galactic nuclei. *Astrophys. J.*, 356:483, June 1990.

[Smi11] Ann Louise Smith. Mathematical analysis of discrete coagulation-fragmentation equations, 2011.

[Smo18] M v Smoluchowski. Versuch einer mathematischen theorie der koagulationskinetik kolloider lösungen. *Z. Phys. Chem. (N F)*, 92U(1):129–168, November 1918.

[Smo27] Marian Smoluchowski. Drei vorträge über diffusion, brownsche molekularbewegung und koagulation von kolloidteilchen. *Pisma Mariana Smoluchowskiego*, 2(1):530–594, 1927.

[SP16] John H Seinfeld and Spyros N Pandis. *Atmospheric chemistry and physics*. Standards Information Network, 3 edition, March 2016.

[Spe09] Joel Spencer. The giant component: The golden anniversary, 2009.

[SYL99] Gerhard Suttner, Harold W Yorke, and Doug N C Lin. Dust coagulation in infalling protostellar envelopes. i. compact grains. *Astrophys. J.*, 524(2):857–866, October 1999.

[VR12] Hanna Vehkamäki and Ilona Riipinen. Thermodynamics and kinetics of atmospheric aerosol particle formation and growth. *Chem. Soc. Rev.*, 41(15):5160–5173, August 2012.

[Wat06] Jonathan A D Wattis. An introduction to mathematical models of coagulation–fragmentation processes: A discrete deterministic mean-field approach. *Physica D*, 222(1-2):1–20, October 2006.